Mon. Not. R. Astron. Soc. **000**, 000–000 (0000) Printed 1 February 2008 (MN LATEX style file v1.4)

# Evidence for a New Class of Extreme UV Sources

Dan Maoz⋆, Eran O. Ofek, and Amotz Shemi
*School of Physics and Astronomy and Wise observatory, The Raymond and Beverly Sackler Faculty of Exact Sciences, Tel-Aviv University, Tel-Aviv 69978, Israel*

1 February 2008



**ABSTRACT**
Most of the sources detected in the extreme ultraviolet (EUV; 100 Å to 600 Å) by the *Rosat/WFC* and *EUVE* all-sky surveys have been identified with active late-type stars and hot white dwarfs that are near enough to escape absorption by interstellar gas. However, about 15% of EUV sources are as of yet unidentified with any optical counterparts. We examine whether the unidentified EUV sources may consist of the same population of late-type stars and white dwarfs. We present $B$ and $R$ photometry of stars in the fields of seven of the unidentified EUV sources. We detect in the optical the entire main-sequence and white-dwarf population out to the greatest distances where they could still avoid absorption. We use colour-magnitude diagrams to demonstrate that, in most of the fields, none of the observed stars have the colours and magnitudes of late-type dwarfs at distances less than 100 pc. Similarly, none are white dwarfs within 500 pc that are hot enough to be EUV-emitters. The unidentified EUV sources we study are not detected in X-rays, while cataclysmic variables, X-ray binaries, and active galactic nuclei generally are. We conclude that some of the EUV sources may be a new class of nearby objects, that are either very faint at optical bands or which mimic the colours and magnitudes of distant late-type stars or cool white dwarfs. One candidate for optically faint objects is isolated old neutron stars, slowly accreting interstellar matter. Such neutron stars are expected to be abundant in the Galaxy, and have not been unambiguously detected.

**Key words:** stars: activity – cataclysmic variables – white dwarfs – stars: neutron – X-rays: stars

## 1 INTRODUCTION

The *ROSAT Wide Field Camera (WFC)* and the *Extreme Ultraviolet Explorer (EUVE)* missions carried out all-sky surveys at extreme-ultraviolet (EUV) wavelengths in 1990-91 and 1992-93, respectively (Pounds et al. 1993; Pye et al. 1995; Malina et al. 1994; Bowyer et al. 1994, 1996). The *EUVE* all-sky survey was carried out in four broad bands, centred at approximately 100 Å, 200 Å, 400 Å, and 600 Å. Simultaneously, a "Deep Survey" with one order of magnitude greater sensitivity was carried out in a $2^\circ \times 180^\circ$ strip of sky along the ecliptic in the 100 Å and 200 Å bands. The *Rosat* WFC all-sky survey was conducted in two EUV bands, centred at about 100 Å and 150 Å. The 100 Å bands in the two all-sky survey experiments had comparable sensitivities.

About 500 EUV sources were detected by each of the surveys, and most of the brightest 300, or so, sources were detected mutually by *EUVE* and *Rosat* (Barber et al. 1995). In ongoing efforts by several groups, about 90% of the *Rosat* EUV sources (Mason et al. 1995) and 65% to 90% (depending on the sample definition) of the *EUVE* sources (Bowyer et al. 1996; Craig et al. 1996b) have been optically identified.

Among the identified sources, about 55% are late-type main-sequence dwarfs with chromospheric activity, and 35% are hot white dwarfs. The remaining 10% are cataclysmic variables (CVs), bright early-type stars, and about 20 bright (13–14 mag) active galactic nuclei (AGNs; Barber et al. 1995; Mason et al. 1995; Marshall, Fruscione, & Carone 1995).

Warwick et al. (1993) showed that the *Rosat* EUV sources which have been identified as white-dwarfs are distributed within the $\sim 100$ pc-radius "Local Bubble" of low-density gas in the interstellar medium (ISM). More distant white dwarfs are undetected in the EUV due to absorption by the higher-density ISM gas. Among the identified active late-type stars, the number/EUV-flux relations fall off as expected for a homogeneously distributed population. In other words, the EUV detection of late-type stars is limited by their faint EUV flux, before they reach the distance of the walls of the Local Bubble. The most distant EUV

⋆ E-mail address: dani@wise.tau.ac.il

sources identified as late-type stars are at 90 pc, for F-type stars, and the distance decreases as one goes to later, less luminous, types, to 40 pc for M-dwarfs. Most EUV-detected M-stars are at about 10 pc (see Warwick et al.1993). It cannot be presently excluded, however, that some of this dependence of maximum detected distance on spectral type is a selection effect of the optical identification programs, which generally concentrate on the brightest objects in a field. For example, EUV sources associated with distant M-stars would more likely remain unidentified than F-stars at the same distance, which are brighter. In any case, even if some late-type stars were bright enough to be detectable in the EUV at larger distances, they would be obscured in the EUV beyond $\sim 100 - 200$ pc, as evidenced by the limiting distances to the identified white dwarfs. It has been speculated that many of the unidentified sources are faint white dwarfs (Warwick et al. 1993; Barber et al. 1995) or late-type stars (Pye et al. 1995).

Most of the ongoing EUV-source identification programs proceed by obtaining optical spectra of the brightest objects within the positional error-circles of the EUV sources. These programs are "positive" in the sense that they aim to complete the identification of as many EUV-sources as possible. EUV sources with optical counterparts fainter than the spectroscopy brightness limit will remain unidentified.

In this paper, we describe the results of an identification program with a "negative" orientation. We have subjectively selected among some of the unidentified EUV sources those that *a priori* appear most difficult to identify. We have chosen those sources that lie in relatively sparse and faint star fields. Our goal is to see whether any of the unidentified EUV sources *cannot* be identified with the common types of optical counterpart. Thus, while the sub-sample of EUV fields we study does not represent statistically any part of the EUV-source population, our program has the potential of identifying new classes of objects with some of the EUV sources (or of showing that such new classes are not yet required).

An exciting possibility for a new class of objects producing some of the unidentified EUV detections is nearby isolated old neutron stars (i.e. neutron stars not in binaries or in supernova remnants, and too old to emit radiation as normal pulsars) accreting material from the ISM (Ostriker, Rees & Silk 1970; Treves & Colpi 1991; Blaes & Madau 1993; Shemi 1995a). The Galaxy is estimated to have $\sim 10^9$ isolated old neutron stars, a population 3-4 orders of magnitude larger than the pulsar population, but which has received little attention. The closest isolated neutron star is likely to be less than $\sim 10$ pc from Earth, and several hundreds are expected within 100 pc. Discussions of the possible spectral properties of isolated neutron stars appear in Treves & Colpi (1991), Blaes & Madau (1993), Madau & Blaes (1994), Zampieri et al. (1995), Nelson et al. (1995), and Shemi (1995a, 1995b). Although the actual spectrum of such objects is not clearly known yet, it is possible that they could be bright enough in the EUV range to be detected by *Rosat* and *EUVE* , but exceedingly faint at optical energies (Shemi 1995a). Indeed, there have recently been reports of two X-ray sources that may be candidates for this class (Stocke et al. 1995; Walter, Wolk,& Neuhauser 1996).

In §2, below, we describe our optical observations of a selection of the EUV source fields, and their reduction. In §3 we present colour-magnitude diagrams for the stars in each field and discuss whether any candidates for optical counterparts exist. We summarize our results in §4.

## 2 OBSERVATIONS AND REDUCTION

For our observations, we selected seven unidentified EUV sources from the compilations of Pounds et al. (1993) and Bowyer et al. (1994, 1996). Apart from the criterion that the fields could be observed from the Northern hemisphere, we generally chose fields that had strong EUV detections, or were detected in more than one band, or with both *Rosat* and *EUVE* . As discussed above, we generally chose sources in sparse fields devoid of bright stars, based on examination of Palomar Sky Survey plates. However, some of the fields are fairly crowded. As noted in more detail for the individual objects in §3, some of the fields we study are not included in the latest compilations of EUV sources detected by *Rosat* (Pye et al. 1995) and *EUVE* (Bowyer et al. 1996). At least one of these (EUVE $2114 + 503$, and probably also EUVE $0807 + 210$) has been erroneously omitted from the catalogs. The others may have been false EUV detections, but they could also be real, and simply below the significance threshold that was set for inclusion in the latest catalogs.

We have searched the recent *Rosat* X-ray All-Sky Survey Bright Source Catalog (Voges et al. 1996), which was conducted at 0.1–2.4 keV simultaneously with the *Rosat* WFC survey, for an X-ray signal coincident to $5'$ with the positions of the unidentified EUV sources. Two of the fields were detected in X-rays, EUVE $0807 + 210$ and EUVE $2053 - 175$. As it happens, these are the two fields in which our analysis, below, points to late-type star candidates, and the candidate positions correspond well to the X-ray source positions. The other five EUV sources were not detected in the X-ray All-Sky Survey. A search of the HEASARC archive of sources from other X-ray missions also does not turn up any documented X-ray sources corresponding to our EUV sources Table 1 lists the fields we have studied, their EUV source parameters, and details of the optical observations.

Observations were carried out with the Wise Observatory 1m telescope and a Tektronix $1024 \times 1024$-pixel back-illuminated CCD. The pixel scale was $0.7''$ per pixel in the direct imaging mode at the Cassegrain focus of the telescope, or $2.08''$ per pixel when imaging with the FOSC instrument (which for the present purposes is simply a focal re-imager). Images of each field were obtained through standard Johnson-Cousins $B$ and $R$ filters. Photometric standard-star fields from Landolt (1992) were also observed throughout each night. Several of the fields were observed on non-photometric nights and were later calibrated by means of brief exposures of the same fields on photometric nights. The photometric solutions yield errors in the terms of the photometric calibration of order 0.01 mag, and an intrinsic scatter of 0.01 to 0.03 mag.

The CCD images were reduced in a standard way using the IRAF[†] package. The positions of the stars on the optical

[†] IRAF (Image Reduction and Analysis Facility) is distributed by the National Optical Astronomy Observatories, which are op-

image were determined with the astrometry task COORDS. The DAOPHOT task (Stetson 1987) was then run on each image to automatically detect and measure the magnitudes of all stars within a $3.5'$ radius of the EUV detection. The various sources of positional error in the *EUVE* and *Rosat* measurements are discussed by Craig et al. (1996b), Bowyer et al. (1996), Pounds et al. (1993), and Pye et al. (1995). The *Rosat* 90%-confidence error circles are listed for each source in the *Rosat* catalogs and are typically $1'$. The *EUVE* 90%-confidence error circles are up to $1.4'$ for objects from the all-sky survey, and up to $2.1'$ for Deep Survey sources. By considering as candidates all stars within $3.5'$ of the EUV detection, we are being highly conservative. Uncertainties in the final $B$ and $R$ magnitudes were found by combining in quadrature the uncertainties in the photometric solution, the scatter of the standard-star measurements around the photometric solution, and the DAOPHOT uncertainties in the PSF fitting of individual stars.

For the typical 15 min exposures, the automatic star detection is complete to stars of at least $B = 21$ mag, for which total errors are 0.1 to 0.25 mag. The $R$ images go to $R = 22$ mag at this level of accuracy. Some of the exposures were shorter or longer (see Table 1), and the detection limits correspondingly shallower or deeper. In all the fields we have studied, all stars that were detected in $B$ were also detected in $R$. On the other hand, many stars are detected in $R$ but not in $B$. In the subsequent analysis we will consider only stars detected in both the $B$ and the $R$ exposures. As we will show in §3, the faint red stars that do not fulfill this condition are unlikely candidates as optical counterparts to the EUV sources.

Tables 2-8 (provided in microfiche form) list, for each field we have analysed, the $B$ and $R$ magnitudes and positions of all the stars in order of increasing distance from the EUV source position. The positions are typically accurate to better than $0.3''$ and can be used, e.g., for planning multi-slit spectroscopy of these fields. The tables are also available electronically on request from the authors.

## 3 ANALYSIS

### 3.1 Method

In this section, we use colour-magnitude diagrams to search for optical counterparts to the EUV sources among the stars we have observed. As explained in §1, the majority ($\sim 90\%$) of *identified* EUV sources are either nearby late-type main-sequence stars (including RS CVn-type stars) or nearby white dwarfs. The remaining 10% of identified EUV sources are composed of CVs (5%), and a handful of early-type stars, X-ray binaries, and AGNs. For each of these populations, we discuss below whether they could be responsible for the unidentified EUV sources we study, and describe the region of the $R$ vs. $B-R$ diagram they occupy. We will then argue that, in fields where none of the stars are in the regions of the colour-magnitude diagram populated by the main known classes of EUV optical counterparts, another class of object must be responsible for the EUV flux.

erated by Aura, Inc., under cooperative agreement with the National Science Foundation.

#### *3.1.1 Active Late-Type Stars*

Active late-type dwarfs nearer than $\sim 100$ pc constitute the majority of EUV sources. To determine the region of the colour-magnitude diagram occupied by them, the relation between absolute magnitude $M_R$, and $B-R$ colour for main-sequence dwarfs is required. For dwarfs of type A0 to M1, the $B-R$ colour-magnitude relation is relatively well known. From Allen (1973) we derive the approximate empirical relation:

$$M_R = 2.8(B-R) + 0.7, \qquad 0 \leq (B-R) \leq 2.8.$$

For types M1 to M4, we estimate from Kirkpatrick et al. (1994):

$$M_R = 6.9(B-R) - 10.78, \qquad 2.8 \leq (B-R) \leq 3.3.$$

For the lowest-mass stars, the relation between magnitude and colour is subject to some uncertainty. In particular, there is little information in the $B$ band, since studies of the faintest and reddest stars are naturally done in the red and infrared parts of the spectrum. However, from Berriman & Reid (1987) we see that for the reddest stars, $(B-R) \approx (V-I)$, up to $(V-I) = 4.5$. (The reddest known stars have $V-I = 4.7$ [Monet et al. 1994] or $V-I \approx 5$ [Kirkpatrick et al. 1994].) Combining this rough equivalence with the relations between $V, R$, and $I$ in Kirkpatrick et al. (1994), we estimate for types M4 to M8:

$$M_R \approx 3(B-R) + 2.1, \qquad 3.3 \leq (B-R) \leq 4.5.$$

In addition to the present uncertainty in these relations, real stars have an intrinsic spread about the relations of order 1-2 magnitudes.

Figures 1-7 show, for every field, an observed colour-magnitude diagram of $R$ vs. $B-R$ for all the sources within $3.5'$ of the EUV source. Also shown (parallel solid and dotted curves) are the colour magnitude relations for a zero-age main sequence (ZAMS) at various distances, as approximated above. At the bottom of the plots we show (marked dashed lines) the $B$ and $R$ detection limits for the exposures of each field. As seen in the figures, the detection limits generally allow us to see all stars to the end of the main sequence out to a few tens pc. At a few 100 pc, we can detect only dwarfs earlier than M. However, Warwick et al. (1993) show that all EUV-sources identified to date with M stars are closer than 40 pc. Since stars have an intrinsic spread of 1-2 magnitudes about the color-magnitude relation, and late-type stars need to be closer than 100 pc to be detected in the EUV, stars that are more than several magnitudes below the 100-pc main sequence cannot be late-type star EUV sources. Similarly, stars that are undetected in $B$ (and hence not plotted in the figures) lie below the diagonal line indicating the $B$ detection limit, and so are not plausible late-type star EUV sources.

Note that any late-type stars detected in the EUV would also be expected to be detected in even a relatively short expoure with the *Rosat* X-ray telescope. The fact that our EUV sources are not detected in the *Rosat* All-Sky-Survey in X-rays (save two EUV sources, which we indeed associate with late-type stars), is an independent argument that our sources are not late-type stars. (This argument does not necessarily hold for white dwarfs, to to their rather "soft" spectra).

#### *3.1.2 White Dwarfs*

The second population that is a main source of EUV detections is hot white dwarfs. The short curves on the left side of the plots show the $R$ vs. $B-R$ relation for white dwarfs at various distances, based on the relation given by Dawson (1986), for white dwarfs with $B-R \leq 0$. Figure 8 shows the distribution of $B-V$ colour of all white-dwarf EUV sources that have been detected by *Rosat* or *EUVE* with available absolute magnitudes. The absolute magnitudes are taken from the compilation by McCook and Sion (1987), and the relation between $M_V$ and $B-V$ is according to Dawson (1986). All white dwarfs that have been detected by either satellite have $B-V \leq 0.13$, which corresponds to $B-R \leq 0$ (Dawson 1986). White dwarfs with $B-R > 0$ are apparently too cool ($T \lesssim 1 \times 10^4$K) to be detected in the EUV. Stars that are much redder than $B-R=0$ cannot be white-dwarf EUV sources. As seen in Figs. 1–7, the detection limits of our observations allow us to see the hot white dwarf population out to $\sim 500$ pc.

#### *3.1.3 Cataclysmic Variables*

CVs constitute about 5% of identified EUV sources. Examination of the properties of CVs that have been identified as EUV sources shows that they have a variety of colours and absolute magnitudes. We therefore cannot exclude that a CV is the EUV source in a given field based solely on the colours and magnitudes of the stars in the field.

However, we note that most of the EUV sources that have been identified with CVs are also X-ray sources. This is seen in Table 9, which lists all CV EUV sources detected by the *EUVE* and *Rosat* surveys and, in the right-hand column, the detection in the *Rosat* X-ray all-sky survey (Voges et al. 1996). Of the 23 CVs detected by either of the EUV surveys 21 are X-ray sources. On the other hand, among the EUV sources we have studied there are 3 *Rosat* X-ray sources: EUVE 0807 + 210 and EUVE 2053 − 175 which we identify below as possible late-type-star EUV sources; and RE 0922+71, where a background quasar unrelated to the EUV source is reponsible for the X-ray emission (see Maoz et al. 1996, and below). The remaining, unidentified, EUV sources are not X-ray sources. This argues that it is unlikely that there are CVs behind all of the unidentified EUV sources. Nevertheless, since there are two examples of X-ray quiet CVs (which were probably active during the *EUVE* survey but quiescent during the *Rosat* surveys), and these have unremarkable colours and magnitudes, we cannot rule out that our EUV sources are CVs.

#### *3.1.4 Other Sources*

About 15% of late-type-star EUV sources that have been identified are chromospherically or coronally active binary systems of the RS CVn and BY Dra-type (Pounds et al. 1993). All the RS-CVn cases, however, are brighter than $V=10$ mag, including some that are very faint in the EUV. Identified BY-Dra binaries are all brighter than $V=11$ mag, but have red colours, so they also fall above the 100 pc ZAMS on the colour magnitude diagram. Stars that cannot be main-sequence late-type-star EUV sources can therefore neither be binaries of these types and be the origin of the EUV flux. Binary systems consisting of a white dwarf and a late-type star can also be EUV sources (Barstow et al. 1994). The EUV emission is dominated by the white dwarf, while the optical light is primarily from the late-type star. We therefore automatically test for sources of this type when we test for late-type-star EUV sources. Several X-ray binaries have been detected in the EUV. Since none of the unidentified EUV sources we study in this paper are *Rosat* All-Sky-Survey X-ray sources, objects of this class do not constitute EUV-source candidates. About 20 bright (13–14 mag) AGNs have been detected in the EUV (Barber et al. 1995; Marshall, Fruscione, & Carone 1995). We have verified that known AGNs are not responsible for the EUV sources studied here. Note also that AGNs have been detected in the EUV only at 100 Å, and these are then always also X-ray sources. Extragalactic objects are not detected at longer EUV wavelengths due to the strong absorption by the ISM of the Galaxy.‡

#### *3.1.5 Absorption and Reddening*

The gas associated with any reddening by dust that affects the position of a star on the colour-magnitude diagram by more than 0.05 mag in $B-R$ would effectively absorb all the EUV radiation from a source. Therefore, if there is a field with no candidate optical counterparts we need not worry whether the colours and magnitudes of some of the stars have been affected by dust. Conversely, fields that do have very red but bright stars could be simply fields with high extinction, rather than fields with nearby late-type stars that are the EUV sources.

### 3.2 Individual Fields

We examine below the colour-magnitude diagram for each of the fields individually. For a star in one of our fields to be a member the same population associated with most EUV sources, it must be either above the ZAMS–100 pc curve (i.e. a late type dwarf closer than 100 pc), or bluer than $B-R=0$ (i.e. a hot white dwarf).

#### *3.2.1 EUVE 0715+141*

This EUV source from the second *EUVE* catalog (Bowyer et al. 1996) was detected independently in three *EUVE* bands – 100 Å, 200 Å, and 400 Å. Even though there are 89 stars within $3.5'$ of the position of this low-latitude ($b=+12°$) source, Fig. 1 shows that none is an obvious candidate. Even given the scatter of real stars around the schematic main-sequence line we have plotted, the nearest of the stars, if they are main sequence dwarfs, are at a distance of over 200 pc, making them unlikely EUV sources. This is especially true given the 400 Å detection, which implies a small distance to the source, given the large ISM absorption cross-section in this band. If the stars in the field are white-dwarfs, they are too red (and hence too cool) to be EUV sources. The

‡ Mild exceptions to this statement are the marginal detections of 1H 1430+423 and PKS 2155−304, both bright and variable BL Lac objects, in the *Rosat* 150 Å band (Pye et al. 1995)

EUV source must therefore be an X-ray-quiet CV, or some new type of EUV source that is optically faint or variable, or that has the colour and magnitude of a distant late-type star but is closer than $\sim 100$ pc.

#### *3.2.2 EUVE 0807+210*

This source was listed as a 200 Å "Deep Survey" detection in the first *EUVE* source catalog (Bowyer et al. 1995), but is not listed in the second catalog (Bowyer et al. 1996). Among the 23 stars within $3.5'$ of the *EUVE* position, there is one (No. 23 in Table 3) that could be a nearby active late-type dwarf. As seen in Fig. 2, it is an 11th mag star with $B - R = 2$, consistent with a K dwarf at a distance of $\sim 100$ pc. Given the scatter of real stars around the main sequence, it could also be as close 50 pc. Its position is $3.2'$ from the *EUVE* position, while the 90% positional error radius is typically $2.1'$. In a search of the *Rosat* X-ray All-Sky-Survey Bright Source Catalog (Voges et al. 1996), we have found a 0.1–2.4 keV X-ray source $0.65'$ north-east of this star (and hence consistent, within the $0.5'$ positional accuracy). Optical spectroscopy can reveal whether this star has characteristics of an active late-type star, in which case it is likely to be the EUV source. If it turns out *not* to be the EUV source then there are no other good candidates in the field, and this is another case of an EUV source with no clear counterparts among the two main classes of EUV emitters.

#### *3.2.3 RE 0847+594*

The *Rosat* 100 Å detection of this source is at the $4.5\sigma$ level, below the $5.5\sigma$ threshold for inclusion in the second *Rosat* WFC catalog (Pye et al. 1995). The *Rosat* data contain a positive signal having a signal consistent with that expected from a point source, but the expected number of spurious $4.5\sigma$ detections over the whole sky is of order 200 (Pye et al. 1995). This source may therefore be a false EUV detection. There are 14 sources within $3.5'$ of the *Rosat* position, none of which appear to be a suitable EUV source candidate (Fig. 3). We note that there is a radio source $82''$ north of the *Rosat* position, with a 6 cm flux of 41 mJy and spectral slope $-0.9$ (Gregory & Condon 1991), possibly associated with objects No. 2 or 5 in Table 4.

#### *3.2.4 RE 0922+710*

An EUV source was detected in this direction by both *Rosat* (at 150 Å; Pounds et al. 1993) and *EUVE* (at 400 Å; Bowyer et al. 1994). It is not included in the second *EUVE* catalog (Bowyer et al. 1996). The *Rosat* detection is at the $3.9\sigma$ level, below the $5.5\sigma$ threshold for inclusion in the second *Rosat* catalog (Pye et al. 1995). There are 18 objects within $3.5'$ of the *Rosat* position. Based on their positions on the colour-magnitude diagram (Fig. 4), none is a suitable EUV source. Maoz et al. (1996) noted that there is a 6 cm radio source and a faint *Rosat* PSPC X-ray source coincident with the bluest object in the field, having $B - R = 0.4$ mag, $R = 18.3$ mag, and lying within the error circles of both the *EUVE* and *Rosat* detections (object No. 3 in Table 5). They used optical spectroscopy to identify this object as a redshift $z = 2.432$ quasar. A 21 cm H I emission measurement in this direction with a $21'$ beam showed that the total H I column density was several orders of magnitude too high for the quasar to be the EUV source (see Maoz et al. 1996, for details). The EUV source in this field therefore remains unidentified, with no candidates among the main classes of EUV sources. A recent repeated observation of this source with *EUVE* (to be described elsewhere) confirms its reality.

#### *3.2.5 EUVE 1636−285*

This is a strong 600 Å source appearing in both the first and second *EUVE* catalogs (Bowyer et al. 1994;1996). Among the 95 sources within $3.5'$ of the *EUVE* position, the most plausible candidate appears to be star No. 52 in Table 6, an $R = 13.3$ mag, $B - R = 2.9$ mag object $2.6'$ from the *EUVE* position. It could be an M star at $\sim 100$ pc. (See Fig. 5). Four other objects in Fig. 5 with $B - R \approx 3$ could also be M stars at $\sim 100$ pc and so could conceivably be the EUV source. On the other hand, one would expect a 600 Å source to be much nearer than 100 pc in order to escape ISM absorption. Furthermore, one would expect an active late-type star that is so strong at 600 Å to have been detected in the shorter-wavelength *EUVE* bands as well. We therefore suspect that none of the detected stars are late-type star or white-dwarf EUV sources. We fail to detect this object in a repeated *EUVE* observation at 100 Å (to be described elsewhere).

#### *3.2.6 EUVE 2053−175*

This source was listed as an unidentified Deep Survey 100 Å emitter in the first *EUVE* catalog (Bowyer et al. 1994), and as an identified $V = 10.4$ mag K star in the second catalog (Bowyer et al. 1996). The identification is described by Craig et al. (1996b), who note it is not conclusive, since no evidence of chromospheric activity or EUV variability are seen. Prior to learning of this identification in the second catalog, we analysed the 38 stars in the short optical exposures within $3.5'$ of the *EUVE* position. We noted that the same star studied by Craig et al. (1996b) (their star "No. 3", star No. 5 in Table 7 in this paper), $82''$ from the *EUVE* position in the first *EUVE* catalog, is a likely candidate EUV source. It has $R = 9.7$ mag and $B - R = 1.3$ mag, consistent with a late G star at 100 pc (see Fig. 6). In a search of the *Rosat* X-ray All-Sky-Survey Bright Source Catalog, we have found a 0.1–2.4 keV X-ray source $15''$ north-west of this star (and hence consistent, within the $0.5'$ positional accuracy). This strengthens the case that it is the EUV source. Star No. 6 in Table 7, separated $91''$ from the *EUVE* position, may be a 13-mag K star at $\sim 100$ pc, and so is also a plausible candidate. Craig et al. (1996b) obtained spectra for two additional stars, No. 3 and No. 4 in Table 7, and assign them spectral types dK1 and dK7, respectively. Our method shows that neither are plausible EUV source candidates, since they are too distant.

#### *3.2.7 EUVE 2114+503*

This is a strong source in the 1st *EUVE* catalog (Bowyer et al. 1994). It is omitted from the 2nd *EUVE* catalog (Bowyer et al. 1996) due to improper subtraction of background from

an adjacent bright white dwarf (A. Fruscione, personal communication). The 100 Å detection is, however, highly significant, and a recent determination of its parameters is given in Craig et al. (1996b). Our deep (3000 s in each band) exposures of this crowded Galactic-plane field ($b = +1^\circ$) show 169 optical sources within $3.5'$ of the *EUVE* position. As seen in Fig. 7, about 20 of these stars have colours and magnitudes consistent with nearby M stars that could be the EUV source. The stars in this direction are almost certainly shifted to this position in the colour-magnitude diagram by strong reddening, so it is also possible that *none* of them is the EUV source. Indeed, Craig et al. (1996b) have obtained spectra of nine stars in the field brighter than $V = 14$ mag, none of which are suitable EUV candidates. Either way, we cannot rule out, based on the current data, that the EUV source in this field is a late-type star. Note also the unusually (relative to the others) blue star (No. 78 in Table 8) with $B - R = 0.14$ mag, $R = 19$ mag, $132''$ from the *EUVE* position. While its place on the diagram argues against its being a white-dwarf EUV source (it is too red and too distant), its colour suggests it is much closer than the other stars in the field, and it deserves further study. It has not been observed by Craig et al. (1996b). A recent repeated observation of this field with *EUVE* (to be described elsewhere) does not reveal any EUV sources, suggesting the source may be a transient EUV emitter.

## 4 SUMMARY

We have presented $B$ and $R$ measurements of stars in the fields of seven unidentified EUV sources detected by *Rosat* and *EUVE* . Using colour-magnitude diagrams, we have argued that, in most of these fields, there are no main-sequence stars near enough to be the EUV source, nor white dwarfs that are hot and near enough. *Many of the unidentified EUV sources are therefore not simply fainter members of these two classes of objects, which are responsible for 90% of identified EUV detections.* The unidentified EUV sources we have studied cannot be X-ray binaries or AGNs, due to the absence of X-ray detections in the *Rosat* X-ray All Sky Survey. It is possible that some or all of the sources we have studied are false detections, although several of them are quite strong, or have been detected in several bands.

We conclude that, if they are real, the objects behind the EUV emission in these fields must be either X-ray quiet CVs or a new class of objects. If they are CVs, they are unusual, since most CVs are X-ray sources. If they constitute a new class, then these objects are either very faint optically, or are an unknown type of nearby Galactic star that mimics the colour and magnitude of a distant late-type dwarf. In the former case, the EUV/optical flux ratio, $\nu F_\nu(150\text{Å})/\nu F_\nu(6500\text{Å}) \gtrsim 100$, i.e. the sources are some kind of extremely hot object, e.g. an isolated old neutron star (see §1). The luminosities of the EUV sources discussed here are $\sim 10^{28} - 10^{31}$ erg s$^{-1}$ (assuming a distance of 10–100 pc), also similar to those predicted for old neutron stars (e.g Madau & Blaes 1994; Shemi 1995a). A third alternative is that the sources emit transiently, and were "turned off" at the time of the optical observations. Obviously, these unidentified EUV sources warrant further study.

**Acknowledgements** We thank K. Anderson, N. Craig, A. Fruscione, P. Madau, T. Mazeh, A. Sternberg, and X. Wu for helpful discussions and suggestions, M. Gardosh for assistance with the observations, and the referee, J. Pye, for constructive and useful comments. Astronomy at Wise Observatory is supported by grants from the Israel Academy of Science. This work was supported by NASA-*EUVE* grant NAG5-2913, and has made use of the NASA/IPAC Extragalactic Database (NED), which is operated by JPL, Caltech, under contract with NASA, the SIMBAD database which is operated at CDS Strasbourg, the HEASARC database at NASA–GSFC, and the *Rosat* archive at MPE-Garching.

## REFERENCES

Allen, C. W. 1973, Astrophysical Quantities, 3rd Edition, (London: Athlone)
Barber, C.R., Warwick, R.S., McGale, P.A., Pye, J.P., Bertram, D. 1995, MNRAS, 273, 93
Barstow, et al. 1994, MNRAS, 270, 499
Berriman, G., Reid, N. 1987, MNRAS, 227, 315
Blaes, O. Madau, P. 1993, ApJ 403, 690
Bowyer, S. et al. 1994, ApJS, 93, 569
Bowyer, S. et al. 1996, ApJS, in press
Cox., D. P., Reynolds, R. J. 1987, ARAA, 25, 303
Craig, N, et al. 1996a, ApJ, 457, L91
Craig, N., et al. 1996b, AJ, in press
Dawson, P.C. 1986, ApJ, 311, 984
Gregory, P. C. Condon, J..J 1991, ApJS 75, 1011
Higdon, J. C. Lingenfelter, R. E. 1990, Ann. Rev. A. Ap. 28, 401
Kirkpatrick, J.D., McGraw, J.T., Hess, T.R., Liebert, J., McCarthy, D.W. 1994, ApJS, 84, 749
Landolt, A.U. 1992, AJ, 104, 340
Madau, P. Blaes, O. 1994, ApJ 423, 748
Malina, R.F., et al. 1994, AJ, 107, 751
Maoz, D. et al. 1996, A&A, 308, 511
Maoz, E. Grindlay, J.E. 1995, ApJ, 444, 183
Marshall, H.L., Fruscione, A., Carone, T.E. 1995, ApJ, 439, 90
Mason, K. O., et al. 1995, MNRAS, 274, 1194
McCook, G. P. Sion, E. M. 1987, ApJS, 65, 603
Monet, D.G., Dahn, C.C., Vrba, F.J., Harris, H.C., Pier, J.R., Luginbuhl, C.B., Ables, H.D. 1992, AJ, 103, 638
Nelson, R.W., Wang, J.C.L., Salpeter, E.E. Wasserman I. 1995, 438, L99
Ostriker, J. P., Rees, M. J., Silk, J. 1970, Astrophys. Lett., 6, 179
Pounds, K.A., et al. 1993, MNRAS, 260, 77
Pye, J.P., et al. 1995, MNRAS, 274, 1165
Shemi, A., 1995a, MNRAS, 275, L7
Shemi, A., 1995b, MNRAS, 275, 115
Stetson, P. B. 1987, PASP, 99, 191
Stocke, J. T., Wang, Q. D., Perlman, E. S., Donahue, M. E., Schachter, J. 1995, AJ, 109, 1199
Treves, A. Colpi, M., 1991, A&A 241, 107
Voges, W., et al. 1996, A&A, in press
Walter, M. F., Wolk, S. J., Neuhauser, R. 1996, Nature, 379, 233
Warwick, R.S., Barber, C.R., Hodgkin, S.T., Pye, J.P. 1993, MNRAS, 262, 289
Zampieri, L., Turolla, R., Zane, S. Treves, A. 1995, ApJ, 439, 849
Zane, S. Turolla, R., Treves, A. 1996, ApJ, in press

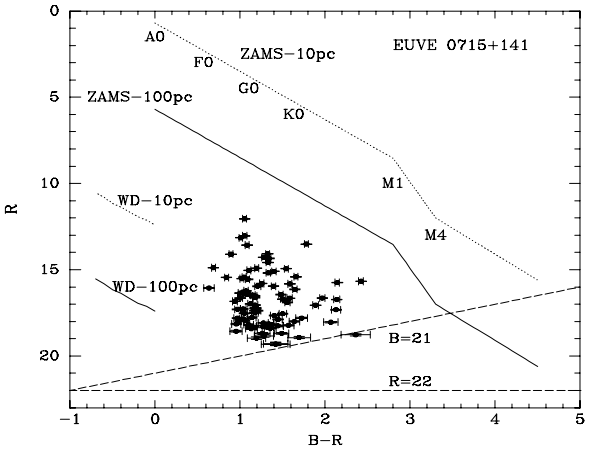


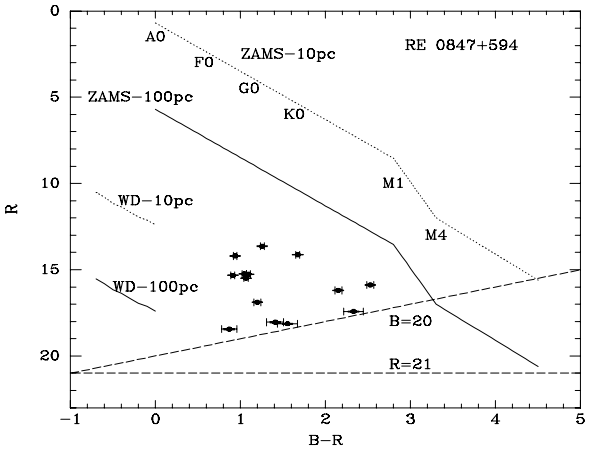


**Figure 1.** (and Figs. 2–7) Colour-magnitude diagrams of $R$ vs. $B-R$ magnitude for stars within $3.5'$ of each of the EUV source positions. The curves marked ZAMS – 10 pc and ZAMS – 100 pc show the approximate locations of the zero-age main sequence at these distances, with some of the spectral types indicated. The curves marked WD – 10 pc and WD – 100 pc show the white dwarf sequence at these distances, for white dwarfs bluer than $B-R=0$. The dashed lines mark the detection limits, in $B$ and $R$, of the optical exposures. To be EUV source candidates, white dwarfs need to be bluer than $B-R=0$ (see Fig. 8), and main sequence dwarfs need to be nearer than $\sim 100$ pc, i.e., above the ZAMS – 100 pc curve. See text for details.

**Figure 3.**

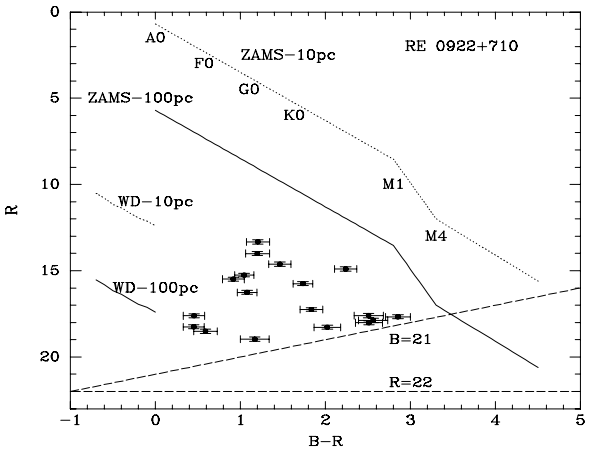


**Figure 4.**

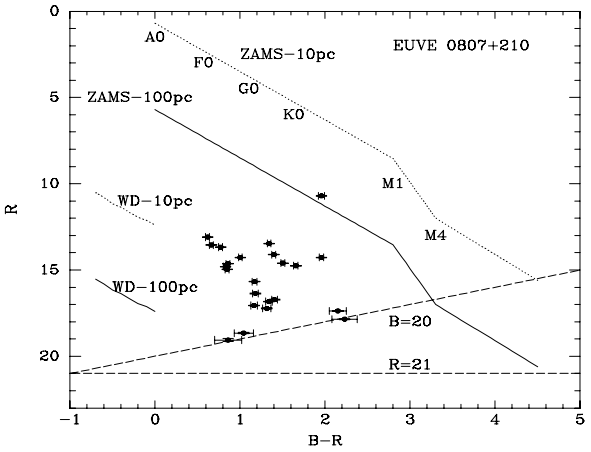


**Figure 2.**

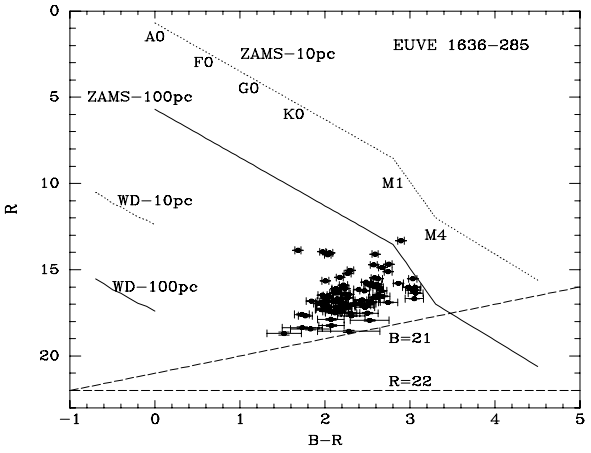


**Figure 5.**

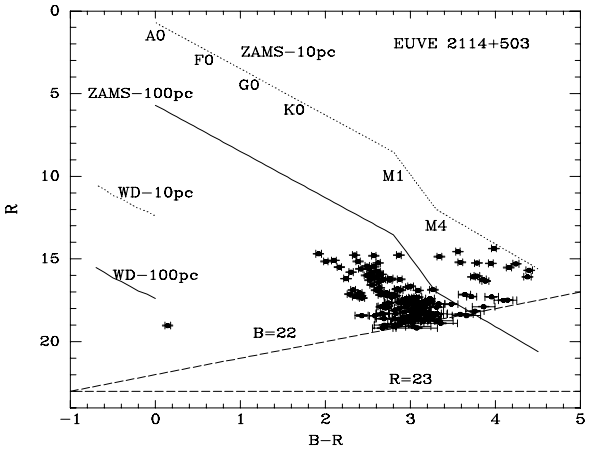


**Figure 7.**

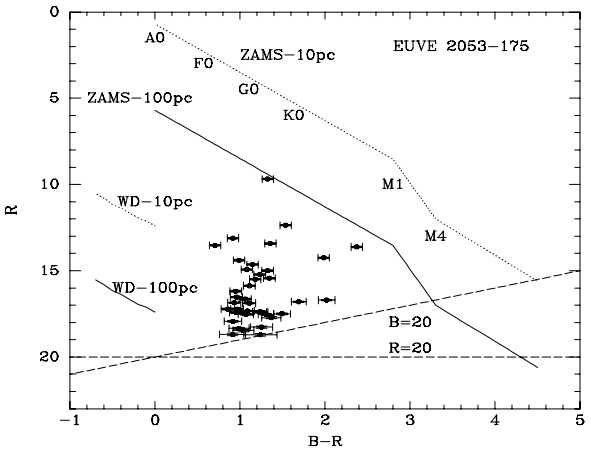


**Figure 6.**

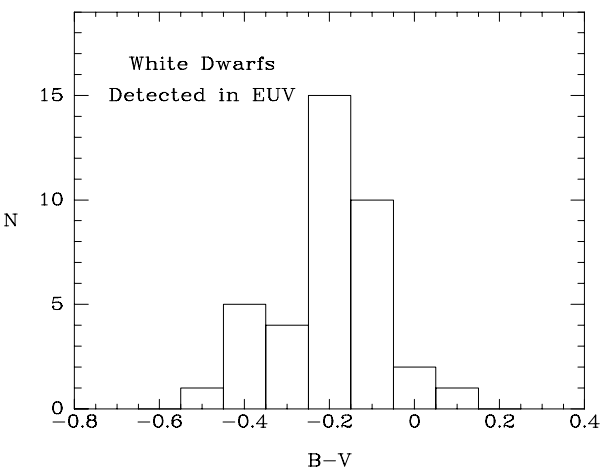


**Figure 8.** Distribution of $B-V$ colour for all white dwarfs with this parameter known, that have been detected in the EUV by *Rosat* or *EUVE* . Only hot white dwarfs, with $B-V \leq 0.13$, have been detected in the EUV.

## Table 1. Unidentified EUV Sources

| EUV Source | EUV Band | R.A. (J2000) | Decl. (J2000) | Galactic $l^{II}$ (degrees) | Galactic $b^{II}$ (degrees) | Optical Observations Date (ddmmyy) | $B$ exp. (sec) | $R$ exp. (sec) |
|---|---|---|---|---|---|---|---|---|
| EUVE 0116−023 | 100Å | 01:16:43 | −02:18:00 | 138 | −64 | 070994 | 900 | 900 |
| EUVE 0138−051 | 200Å | 01:38:31 | −05:09:24 | 152 | −65 | 130894 | 720 | 1200 |
| EUVE 0715+141 | 100Å, 200Å, 400Å | 07:15:50 | +14:10:18 | 203 | +12 | 250395 | 1200 | 600 |
| EUVE 0807+210 | 200Å | 08:07:59 | +21:04:12 | 201 | +26 | 251194 | 300 | 300 |
| RE 0847+594 | 100Å | 08:47:13 | +59:47:00 | 157 | +38 | 190495 | 300 | 300 |
| RE 0922+710 | 150Å, EUVE 400Å | 09:22:29 | +71:10:06 | 142 | +37 | 010794 | 2400 | 1200 |
| EUVE 2053−175 | 100Å | 20:53:35 | −17:33:54 | 30 | −35 | 070994 | 240 | 150 |
| EUVE 2114+503 | 100Å | 21:14:41 | +50:18:12 | 92 | + 1 | 130894 | 3000 | 3000 |
| RE 2303+212 | 150Å | 23:03:04 | +21:20:32 | 92 | −35 | 130894 | 500 | 300 |

## Table 2. EUVE 0116−023

| No. | Sep. arcsec | $\Delta\alpha$ arcsec | $\Delta\delta$ arcsec | $B$ mag | $\sigma$ | $R$ mag | $\sigma$ | $B-R$ mag | $\sigma$ |
|---|---|---|---|---|---|---|---|---|---|
| 1 | 103.4 | −32.8 | 98.0 | 15.091 | 0.053 | 13.640 | 0.040 | 1.451 | 0.066 |
| 2 | 139.5 | 47.2 | 131.3 | 14.295 | 0.053 | 13.283 | 0.040 | 1.012 | 0.066 |
| 3 | 146.3 | −120.5 | 82.9 | 11.738 | 0.053 | 10.930 | 0.040 | 0.808 | 0.066 |
| 4 | 196.6 | 130.8 | 146.8 | 18.729 | 0.064 | 16.176 | 0.040 | 2.553 | 0.075 |
| 5 | 201.2 | −91.4 | −179.3 | 17.640 | 0.056 | 16.817 | 0.040 | 0.823 | 0.069 |

Notes to Table 2.

Positions relative to $\alpha = 01:16:43$, $\delta = -02:18:00$ (J2000)

## TABLE 3. EUVE 0138−051

| No. | Sep. | $\Delta\alpha$ | $\Delta\delta$ | $B$ | | $R$ | | $B-R$ | |
|---|---|---|---|---|---|---|---|---|---|
| | arcsec | arcsec | arcsec | mag | $\sigma$ | mag | $\sigma$ | mag | $\sigma$ |
| 1 | 41.7 | 40.6 | −9.4 | 14.256 | 0.018 | 13.315 | 0.018 | 0.941 | 0.026 |
| 2 | 50.2 | −22.1 | 45.1 | 13.920 | 0.018 | 12.986 | 0.018 | 0.934 | 0.026 |
| 3 | 52.2 | 8.5 | 51.5 | 20.159 | 0.079 | 17.683 | 0.019 | 2.476 | 0.081 |
| 4 | 85.0 | 43.8 | −72.9 | 20.437 | 0.099 | 18.550 | 0.022 | 1.887 | 0.101 |
| 5 | 126.4 | −72.9 | 103.2 | 18.915 | 0.036 | 17.667 | 0.019 | 1.248 | 0.041 |
| 6 | 142.9 | −49.6 | −134.0 | 17.257 | 0.020 | 16.018 | 0.018 | 1.239 | 0.027 |
| 7 | 154.7 | −151.0 | −33.6 | 17.084 | 0.020 | 15.584 | 0.018 | 1.500 | 0.027 |
| 8 | 162.8 | −132.5 | 94.6 | 18.187 | 0.024 | 16.541 | 0.018 | 1.646 | 0.030 |
| 9 | 164.4 | −163.7 | −14.3 | 19.711 | 0.052 | 17.328 | 0.019 | 2.383 | 0.056 |
| 10 | 188.7 | 173.0 | −75.4 | 18.037 | 0.065 | 16.553 | 0.097 | 1.484 | 0.116 |
| 11 | 190.6 | −79.5 | −173.2 | 20.845 | 0.134 | 18.364 | 0.021 | 2.481 | 0.136 |
| 12 | 207.2 | 199.6 | 55.8 | 17.588 | 0.020 | 15.602 | 0.018 | 1.986 | 0.027 |

Notes to Table 3.

Positions relative to $\alpha = 01:38:31$, $\delta = -05:09:24$ (J2000)

# Table 4. EUVE 0715+141

| No. | Sep. | $\Delta\alpha$ | $\Delta\delta$ | $B$ | | $R$ | | $B-R$ | |
|---|---|---|---|---|---|---|---|---|---|
| | arcsec | arcsec | arcsec | mag | $\sigma$ | mag | $\sigma$ | mag | $\sigma$ |
| 1 | 16.8 | 16.7 | 1.6 | 19.295 | 0.042 | 18.193 | 0.036 | 1.101 | 0.055 |
| 2 | 20.8 | 17.5 | −11.4 | 17.354 | 0.019 | 16.353 | 0.016 | 1.000 | 0.025 |
| 3 | 21.8 | 18.2 | 12.0 | 18.454 | 0.024 | 16.897 | 0.021 | 1.556 | 0.032 |
| 4 | 34.5 | −21.4 | 27.1 | 21.133 | 0.160 | 18.773 | 0.065 | 2.359 | 0.172 |
| 5 | 35.3 | −19.2 | −29.6 | 18.921 | 0.029 | 17.922 | 0.032 | 0.998 | 0.044 |
| 6 | 38.1 | 17.5 | −33.9 | 14.987 | 0.017 | 14.094 | 0.014 | 0.892 | 0.023 |
| 7 | 46.8 | 13.4 | 44.8 | 18.311 | 0.025 | 17.275 | 0.021 | 1.035 | 0.033 |
| 8 | 50.4 | −23.3 | 44.7 | 20.628 | 0.116 | 18.932 | 0.067 | 1.695 | 0.134 |
| 9 | 71.0 | −65.9 | −26.3 | 17.163 | 0.029 | 15.955 | 0.022 | 1.207 | 0.036 |
| 10 | 72.0 | −33.9 | −63.6 | 15.565 | 0.018 | 14.286 | 0.014 | 1.278 | 0.023 |
| 11 | 75.8 | 17.6 | −73.7 | 16.644 | 0.018 | 15.554 | 0.015 | 1.089 | 0.023 |
| 12 | 77.1 | 11.5 | −76.3 | 18.914 | 0.034 | 17.775 | 0.035 | 1.138 | 0.049 |
| 13 | 77.4 | −43.2 | 64.2 | 19.544 | 0.040 | 18.179 | 0.041 | 1.364 | 0.057 |
| 14 | 78.4 | 6.1 | −78.2 | 17.773 | 0.021 | 16.832 | 0.020 | 0.940 | 0.029 |
| 15 | 82.5 | 45.2 | −69.0 | 15.572 | 0.018 | 14.885 | 0.014 | 0.686 | 0.023 |
| 16 | 82.8 | 24.4 | −79.1 | 19.701 | 0.051 | 18.255 | 0.045 | 1.445 | 0.068 |
| 17 | 86.2 | 78.4 | −35.8 | 13.105 | 0.017 | 12.051 | 0.015 | 1.053 | 0.022 |
| 18 | 87.2 | −84.6 | −21.0 | 18.581 | 0.027 | 17.529 | 0.023 | 1.051 | 0.035 |
| 19 | 87.5 | −37.1 | −79.3 | 15.906 | 0.019 | 14.577 | 0.015 | 1.328 | 0.024 |
| 20 | 91.6 | −91.2 | −9.0 | 19.450 | 0.048 | 17.321 | 0.025 | 2.128 | 0.054 |
| 21 | 96.0 | −43.3 | −85.7 | 14.090 | 0.019 | 13.034 | 0.014 | 1.055 | 0.024 |
| 22 | 96.8 | −86.1 | −44.2 | 18.609 | 0.026 | 16.642 | 0.017 | 1.966 | 0.031 |
| 23 | 98.9 | 98.8 | −4.9 | 17.297 | 0.018 | 16.226 | 0.016 | 1.070 | 0.024 |
| 24 | 98.9 | −94.5 | −29.0 | 17.645 | 0.020 | 16.643 | 0.018 | 1.001 | 0.027 |
| 25 | 99.6 | 2.5 | 99.5 | 19.006 | 0.031 | 17.950 | 0.040 | 1.055 | 0.050 |
| 26 | 99.9 | −66.3 | 74.7 | 19.752 | 0.050 | 18.396 | 0.047 | 1.355 | 0.069 |
| 27 | 100.8 | 53.1 | 85.7 | 16.291 | 0.018 | 15.451 | 0.015 | 0.839 | 0.023 |
| 28 | 103.9 | −82.6 | 62.9 | 16.147 | 0.018 | 15.041 | 0.015 | 1.105 | 0.023 |
| 29 | 107.9 | −72.7 | −79.7 | 16.109 | 0.019 | 14.914 | 0.015 | 1.194 | 0.024 |
| 30 | 111.2 | −103.7 | 40.2 | 19.059 | 0.032 | 17.655 | 0.031 | 1.403 | 0.045 |
| 31 | 112.2 | 64.1 | −92.0 | 18.203 | 0.023 | 16.701 | 0.017 | 1.501 | 0.028 |
| 32 | 112.4 | 107.2 | 33.8 | 19.405 | 0.039 | 18.266 | 0.039 | 1.138 | 0.055 |
| 33 | 113.2 | −109.8 | −27.4 | 19.576 | 0.056 | 18.304 | 0.063 | 1.271 | 0.084 |
| 34 | 114.4 | −29.5 | 110.6 | 20.128 | 0.081 | 18.848 | 0.077 | 1.279 | 0.112 |
| 35 | 115.0 | −72.4 | −89.3 | 20.166 | 0.080 | 18.972 | 0.070 | 1.193 | 0.106 |
| 36 | 119.6 | 119.5 | −2.2 | 18.946 | 0.028 | 17.058 | 0.020 | 1.887 | 0.034 |
| 37 | 122.1 | 78.5 | −93.5 | 15.291 | 0.018 | 13.510 | 0.014 | 1.780 | 0.023 |
| 38 | 124.3 | 51.2 | −113.2 | 19.099 | 0.039 | 18.144 | 0.036 | 0.954 | 0.053 |
| 39 | 131.7 | 14.8 | −130.8 | 17.069 | 0.019 | 15.412 | 0.015 | 1.656 | 0.024 |
| 40 | 131.9 | −93.5 | −93.1 | 18.233 | 0.023 | 16.649 | 0.017 | 1.583 | 0.029 |
| 41 | 132.7 | 115.8 | −64.8 | 18.574 | 0.029 | 17.367 | 0.023 | 1.206 | 0.037 |
| 42 | 132.7 | 131.9 | 14.3 | 17.786 | 0.021 | 16.614 | 0.018 | 1.171 | 0.027 |
| 43 | 133.8 | 88.7 | −100.1 | 18.773 | 0.031 | 17.802 | 0.028 | 0.970 | 0.042 |
| 44 | 133.9 | 63.0 | 118.2 | 20.109 | 0.079 | 18.041 | 0.037 | 2.067 | 0.087 |
| 45 | 138.9 | −53.4 | −128.3 | 19.366 | 0.043 | 18.094 | 0.041 | 1.271 | 0.059 |
| 46 | 140.0 | −65.3 | 123.8 | 18.264 | 0.023 | 17.293 | 0.021 | 0.970 | 0.032 |

TABLE 4. (continued)

| No. | Sep. | $\Delta\alpha$ | $\Delta\delta$ | $B$ | | $R$ | | $B-R$ | |
|---|---|---|---|---|---|---|---|---|---|
| | arcsec | arcsec | arcsec | mag | $\sigma$ | mag | $\sigma$ | mag | $\sigma$ |
| 47 | 142.0 | −83.3 | 114.9 | 19.528 | 0.058 | 17.803 | 0.039 | 1.724 | 0.069 |
| 48 | 143.4 | −3.3 | 143.4 | 19.330 | 0.040 | 17.882 | 0.027 | 1.447 | 0.048 |
| 49 | 145.2 | 21.2 | 143.7 | 17.054 | 0.018 | 15.799 | 0.015 | 1.254 | 0.024 |
| 50 | 148.8 | 139.9 | 50.7 | 20.176 | 0.068 | 18.687 | 0.051 | 1.488 | 0.085 |
| 51 | 152.9 | −146.2 | 44.7 | 17.468 | 0.020 | 16.384 | 0.016 | 1.083 | 0.025 |
| 52 | 154.5 | 49.2 | −146.5 | 18.675 | 0.028 | 17.500 | 0.028 | 1.174 | 0.039 |
| 53 | 155.6 | −118.8 | −100.5 | 18.554 | 0.029 | 17.379 | 0.023 | 1.174 | 0.037 |
| 54 | 156.9 | 156.9 | −1.6 | 18.103 | 0.024 | 16.980 | 0.019 | 1.122 | 0.031 |
| 55 | 157.2 | −68.9 | 141.3 | 17.785 | 0.020 | 16.139 | 0.016 | 1.645 | 0.026 |
| 56 | 157.6 | −103.1 | −119.2 | 15.405 | 0.020 | 14.081 | 0.015 | 1.323 | 0.025 |
| 57 | 159.7 | −35.5 | −155.7 | 18.226 | 0.024 | 17.049 | 0.021 | 1.176 | 0.032 |
| 58 | 162.4 | −50.2 | −154.4 | 16.495 | 0.020 | 15.098 | 0.015 | 1.396 | 0.025 |
| 59 | 163.1 | −12.7 | −162.6 | 17.349 | 0.020 | 15.955 | 0.015 | 1.393 | 0.025 |
| 60 | 163.4 | −160.9 | 28.8 | 14.161 | 0.018 | 13.152 | 0.014 | 1.008 | 0.023 |
| 61 | 164.6 | 108.6 | −123.6 | 17.687 | 0.020 | 16.514 | 0.016 | 1.172 | 0.025 |
| 62 | 168.2 | 150.1 | −76.0 | 16.542 | 0.018 | 15.519 | 0.015 | 1.022 | 0.023 |
| 63 | 168.5 | 168.1 | 12.0 | 19.797 | 0.056 | 18.227 | 0.036 | 1.569 | 0.066 |
| 64 | 174.1 | 9.7 | −173.8 | 18.093 | 0.023 | 15.669 | 0.016 | 2.423 | 0.028 |
| 65 | 177.4 | −87.0 | −154.6 | 20.739 | 0.144 | 19.319 | 0.088 | 1.419 | 0.169 |
| 66 | 179.7 | 172.2 | −51.2 | 15.685 | 0.017 | 14.343 | 0.014 | 1.341 | 0.023 |
| 67 | 182.5 | −181.6 | −17.2 | 16.478 | 0.019 | 15.430 | 0.015 | 1.047 | 0.024 |
| 68 | 182.9 | −41.0 | −178.3 | 17.410 | 0.021 | 16.346 | 0.016 | 1.063 | 0.026 |
| 69 | 184.9 | 46.0 | 179.1 | 16.693 | 0.061 | 16.059 | 0.016 | 0.633 | 0.063 |
| 70 | 184.9 | 70.8 | 170.8 | 17.889 | 0.021 | 15.745 | 0.015 | 2.143 | 0.026 |
| 71 | 185.9 | −108.9 | −150.7 | 16.515 | 0.020 | 15.183 | 0.015 | 1.331 | 0.025 |
| 72 | 187.2 | 41.9 | −182.4 | 18.863 | 0.030 | 16.726 | 0.017 | 2.136 | 0.035 |
| 73 | 187.6 | 90.3 | 164.5 | 16.489 | 0.018 | 14.946 | 0.015 | 1.542 | 0.023 |
| 74 | 189.2 | 179.2 | 60.7 | 17.920 | 0.021 | 16.440 | 0.017 | 1.479 | 0.027 |
| 75 | 190.7 | −39.4 | −186.6 | 19.483 | 0.042 | 18.146 | 0.040 | 1.336 | 0.057 |
| 76 | 191.7 | 155.2 | −112.6 | 19.520 | 0.051 | 18.566 | 0.049 | 0.953 | 0.071 |
| 77 | 193.2 | −192.3 | −18.8 | 17.409 | 0.019 | 15.823 | 0.016 | 1.585 | 0.025 |
| 78 | 193.8 | −167.0 | 98.4 | 18.406 | 0.022 | 17.226 | 0.021 | 1.179 | 0.031 |
| 79 | 195.0 | −5.7 | −194.9 | 14.656 | 0.020 | 13.573 | 0.015 | 1.082 | 0.025 |
| 80 | 195.5 | 40.3 | −191.3 | 19.956 | 0.068 | 18.694 | 0.059 | 1.261 | 0.090 |
| 81 | 195.5 | −195.5 | 4.3 | 19.551 | 0.038 | 18.417 | 0.056 | 1.133 | 0.068 |
| 82 | 196.2 | 6.4 | −196.1 | 18.893 | 0.033 | 17.853 | 0.030 | 1.039 | 0.045 |
| 83 | 197.2 | 15.1 | 196.6 | 19.057 | 0.034 | 17.555 | 0.027 | 1.501 | 0.044 |
| 84 | 203.3 | −179.6 | 95.2 | 19.643 | 0.050 | 18.004 | 0.035 | 1.638 | 0.061 |
| 85 | 203.6 | 155.9 | 131.0 | 19.673 | 0.046 | 18.347 | 0.046 | 1.325 | 0.065 |
| 86 | 204.9 | 144.6 | 145.3 | 17.512 | 0.025 | 16.431 | 0.024 | 1.080 | 0.035 |
| 87 | 206.5 | 122.2 | 166.5 | 17.631 | 0.020 | 16.477 | 0.017 | 1.153 | 0.026 |
| 88 | 207.6 | 183.8 | 96.4 | 18.432 | 0.023 | 17.252 | 0.021 | 1.179 | 0.031 |
| 89 | 210.4 | 78.8 | 195.1 | 20.721 | 0.098 | 19.301 | 0.107 | 1.419 | 0.145 |

Notes to Table 4.

Positions relative to $\alpha = 07:15:50$, $\delta = +14:10:18$ (J2000)

## Table 5. EUVE 0807+210

| No. | Sep. | $\Delta\alpha$ | $\Delta\delta$ | $B$ | | $R$ | | $B-R$ | |
|---|---|---|---|---|---|---|---|---|---|
| | arcsec | arcsec | arcsec | mag | $\sigma$ | mag | $\sigma$ | mag | $\sigma$ |
| 1 | 43.8 | 6.2 | 43.3 | 16.100 | 0.019 | 14.598 | 0.014 | 1.502 | 0.024 |
| 2 | 72.2 | −45.8 | 55.9 | 15.813 | 0.018 | 14.965 | 0.014 | 0.848 | 0.023 |
| 3 | 74.7 | −23.2 | −71.0 | 18.126 | 0.029 | 16.721 | 0.017 | 1.405 | 0.033 |
| 4 | 83.6 | 83.6 | 2.6 | 13.707 | 0.017 | 13.090 | 0.014 | 0.617 | 0.022 |
| 5 | 90.5 | −88.3 | 19.5 | 14.215 | 0.017 | 13.553 | 0.014 | 0.662 | 0.022 |
| 6 | 95.8 | −92.0 | 26.7 | 14.807 | 0.017 | 13.466 | 0.014 | 1.341 | 0.022 |
| 7 | 96.9 | −12.0 | 96.1 | 19.916 | 0.125 | 19.057 | 0.095 | 0.859 | 0.157 |
| 8 | 105.1 | −24.6 | −102.2 | 18.542 | 0.043 | 17.229 | 0.019 | 1.313 | 0.047 |
| 9 | 105.3 | 91.8 | −51.5 | 15.272 | 0.017 | 14.270 | 0.014 | 1.002 | 0.022 |
| 10 | 106.9 | 103.3 | 27.4 | 19.701 | 0.104 | 18.659 | 0.042 | 1.042 | 0.113 |
| 11 | 114.0 | 23.5 | −111.6 | 18.225 | 0.032 | 17.060 | 0.018 | 1.165 | 0.037 |
| 12 | 129.7 | −89.6 | −93.8 | 16.410 | 0.020 | 14.754 | 0.015 | 1.656 | 0.025 |
| 13 | 130.1 | −125.6 | −34.2 | 15.632 | 0.018 | 14.804 | 0.014 | 0.828 | 0.023 |
| 14 | 135.9 | −135.2 | 13.7 | 15.494 | 0.018 | 14.637 | 0.014 | 0.857 | 0.023 |
| 15 | 137.1 | 113.9 | 76.3 | 20.082 | 0.147 | 17.852 | 0.023 | 2.230 | 0.149 |
| 16 | 143.2 | −76.3 | −121.2 | 17.541 | 0.026 | 16.361 | 0.016 | 1.180 | 0.031 |
| 17 | 143.8 | −134.4 | 51.2 | 18.169 | 0.034 | 16.831 | 0.019 | 1.338 | 0.039 |
| 18 | 153.9 | −146.4 | −47.3 | 19.522 | 0.097 | 17.372 | 0.021 | 2.150 | 0.099 |
| 19 | 170.9 | −65.4 | −157.9 | 16.844 | 0.022 | 15.675 | 0.015 | 1.169 | 0.027 |
| 20 | 178.6 | 158.7 | −81.8 | 14.446 | 0.017 | 13.675 | 0.014 | 0.771 | 0.022 |
| 21 | 182.2 | −67.3 | −169.3 | 15.508 | 0.017 | 14.112 | 0.014 | 1.396 | 0.022 |
| 22 | 189.9 | −133.1 | −135.4 | 16.231 | 0.019 | 14.274 | 0.014 | 1.957 | 0.024 |
| 23 | 193.2 | 171.0 | 89.9 | 12.657 | 0.017 | 10.700 | 0.032 | 1.957 | 0.037 |

Notes to Table 5.

Positions relative to $\alpha = 08:07:59$, $\delta = +21:04:12$ (J2000)

## TABLE 6. RE 0847+594

| No. | Sep. | $\Delta\alpha$ | $\Delta\delta$ | $B$ | | $R$ | | $B-R$ | |
|---|---|---|---|---|---|---|---|---|---|
| | arcsec | arcsec | arcsec | mag | $\sigma$ | mag | $\sigma$ | mag | $\sigma$ |
| 1 | 51.6 | 43.3 | 28.0 | 19.750 | 0.114 | 17.421 | 0.021 | 2.329 | 0.116 |
| 2 | 96.0 | 87.5 | 39.5 | 16.235 | 0.019 | 15.326 | 0.014 | 0.909 | 0.024 |
| 3 | 109.6 | 76.3 | −78.6 | 14.891 | 0.017 | 13.636 | 0.015 | 1.255 | 0.023 |
| 4 | 116.4 | −115.8 | 12.2 | 16.354 | 0.018 | 15.261 | 0.015 | 1.093 | 0.023 |
| 5 | 120.9 | 120.0 | 15.0 | 16.288 | 0.020 | 15.244 | 0.014 | 1.044 | 0.024 |
| 6 | 127.5 | 44.8 | −119.3 | 15.138 | 0.017 | 14.202 | 0.014 | 0.936 | 0.022 |
| 7 | 143.7 | −81.7 | −118.2 | 19.682 | 0.114 | 18.129 | 0.031 | 1.553 | 0.118 |
| 8 | 143.8 | −125.0 | −71.0 | 18.407 | 0.039 | 15.882 | 0.015 | 2.525 | 0.042 |
| 9 | 149.4 | 148.5 | −16.1 | 18.089 | 0.038 | 16.891 | 0.017 | 1.198 | 0.041 |
| 10 | 160.5 | −146.1 | −66.3 | 18.347 | 0.038 | 16.197 | 0.015 | 2.150 | 0.041 |
| 11 | 167.0 | −142.1 | 87.9 | 19.452 | 0.096 | 18.045 | 0.026 | 1.407 | 0.099 |
| 12 | 168.5 | −113.0 | −124.9 | 19.308 | 0.082 | 18.441 | 0.037 | 0.867 | 0.090 |
| 13 | 193.6 | 188.1 | 45.7 | 16.550 | 0.021 | 15.485 | 0.015 | 1.065 | 0.026 |
| 14 | 205.4 | −151.8 | 138.5 | 15.805 | 0.019 | 14.132 | 0.014 | 1.673 | 0.024 |

Notes to Table 6.

Positions relative to $\alpha = 08:47:13$, $\delta = +59:47:00$ (J2000)

## TABLE 7. EUVE 0922+711

| No. | Sep. | $\Delta\alpha$ | $\Delta\delta$ | $B$ | | $R$ | | $B-R$ | |
|---|---|---|---|---|---|---|---|---|---|
| | arcsec | arcsec | arcsec | mag | $\sigma$ | mag | $\sigma$ | mag | $\sigma$ |
| 1 | 23.7 | −21.2 | −10.6 | 20.442 | 0.124 | 17.881 | 0.117 | 2.561 | 0.171 |
| 2 | 28.4 | −26.3 | 10.7 | 17.332 | 0.039 | 16.255 | 0.109 | 1.077 | 0.116 |
| 3 | 29.2 | 5.3 | −28.7 | 18.700 | 0.052 | 18.251 | 0.111 | 0.449 | 0.122 |
| 4 | 48.8 | −41.6 | 25.6 | 17.482 | 0.036 | 15.749 | 0.111 | 1.733 | 0.116 |
| 5 | 86.1 | −77.1 | −38.3 | 20.140 | 0.116 | 18.972 | 0.122 | 1.168 | 0.168 |
| 6 | 94.0 | −9.3 | 93.6 | 20.526 | 0.112 | 18.017 | 0.112 | 2.509 | 0.158 |
| 7 | 100.8 | −45.0 | −90.2 | 20.527 | 0.095 | 17.676 | 0.111 | 2.851 | 0.146 |
| 8 | 103.8 | 54.4 | −88.4 | 19.080 | 0.072 | 17.246 | 0.111 | 1.834 | 0.132 |
| 9 | 142.8 | −142.5 | 8.7 | 16.405 | 0.052 | 15.490 | 0.116 | 0.915 | 0.127 |
| 10 | 144.6 | 139.9 | −36.4 | 15.201 | 0.084 | 14.002 | 0.112 | 1.199 | 0.140 |
| 11 | 160.5 | −0.6 | −160.5 | 16.294 | 0.029 | 15.252 | 0.109 | 1.042 | 0.113 |
| 12 | 166.8 | −128.5 | 106.5 | 17.139 | 0.053 | 14.902 | 0.119 | 2.237 | 0.130 |
| 13 | 184.9 | 171.6 | −68.7 | 16.083 | 0.058 | 14.621 | 0.117 | 1.462 | 0.131 |
| 14 | 187.1 | 117.9 | 145.4 | 20.101 | 0.120 | 17.595 | 0.124 | 2.506 | 0.172 |
| 15 | 192.7 | −118.1 | −152.2 | 19.093 | 0.061 | 18.506 | 0.124 | 0.587 | 0.138 |
| 16 | 199.8 | −91.6 | −177.5 | 18.067 | 0.040 | 17.614 | 0.118 | 0.453 | 0.125 |
| 17 | 202.5 | 181.7 | −89.2 | 14.530 | 0.047 | 13.326 | 0.127 | 1.204 | 0.135 |
| 18 | 204.4 | 45.1 | −199.3 | 20.298 | 0.108 | 18.278 | 0.113 | 2.020 | 0.156 |

Notes to Table 7.

Positions relative to $\alpha = 09:22:29$, $\delta = +71:10:06$ (J2000)

# Table 8. EUVE 2053−175

| No. | Sep. | $\Delta\alpha$ | $\Delta\delta$ | $B$ | | $R$ | | $B-R$ | |
|---|---|---|---|---|---|---|---|---|---|
| | arcsec | arcsec | arcsec | mag | $\sigma$ | mag | $\sigma$ | mag | $\sigma$ |
| 1 | 37.0 | 35.9 | −8.9 | 18.838 | 0.079 | 17.532 | 0.045 | 1.306 | 0.091 |
| 2 | 38.5 | 32.9 | 19.9 | 17.788 | 0.060 | 16.857 | 0.044 | 0.931 | 0.075 |
| 3 | 69.5 | −24.9 | −64.9 | 16.229 | 0.054 | 14.246 | 0.040 | 1.983 | 0.067 |
| 4 | 72.3 | 26.0 | −67.5 | 16.983 | 0.055 | 15.873 | 0.041 | 1.110 | 0.069 |
| 5 | 81.9 | −75.9 | −30.8 | 11.007 | 0.053 | 9.683 | 0.040 | 1.324 | 0.066 |
| 6 | 91.2 | −55.8 | 72.2 | 15.993 | 0.054 | 13.622 | 0.040 | 2.371 | 0.067 |
| 7 | 94.0 | 34.9 | −87.2 | 19.510 | 0.106 | 18.471 | 0.059 | 1.039 | 0.122 |
| 8 | 106.2 | 19.3 | 104.4 | 18.987 | 0.087 | 17.495 | 0.049 | 1.492 | 0.100 |
| 9 | 107.8 | 63.4 | 87.3 | 16.011 | 0.054 | 14.933 | 0.040 | 1.078 | 0.067 |
| 10 | 113.9 | −14.9 | −112.9 | 17.700 | 0.059 | 16.641 | 0.042 | 1.059 | 0.073 |
| 11 | 116.8 | −108.4 | −43.6 | 16.321 | 0.054 | 14.998 | 0.040 | 1.323 | 0.067 |
| 12 | 121.4 | 77.1 | −93.8 | 14.236 | 0.053 | 13.531 | 0.040 | 0.705 | 0.066 |
| 13 | 123.6 | 120.8 | 26.1 | 18.419 | 0.070 | 17.335 | 0.044 | 1.084 | 0.083 |
| 14 | 125.3 | −121.4 | 30.9 | 15.789 | 0.054 | 14.644 | 0.040 | 1.145 | 0.067 |
| 15 | 126.2 | −72.5 | 103.2 | 13.899 | 0.053 | 12.364 | 0.040 | 1.535 | 0.066 |
| 16 | 128.3 | 121.6 | 41.0 | 16.776 | 0.056 | 15.433 | 0.040 | 1.343 | 0.069 |
| 17 | 129.1 | 128.3 | −14.9 | 17.990 | 0.065 | 16.883 | 0.041 | 1.107 | 0.077 |
| 18 | 130.0 | −100.1 | 82.9 | 16.449 | 0.054 | 15.218 | 0.040 | 1.231 | 0.067 |
| 19 | 134.1 | 71.4 | −113.5 | 18.721 | 0.088 | 16.704 | 0.042 | 2.017 | 0.097 |
| 20 | 137.3 | 137.1 | −6.8 | 19.326 | 0.105 | 18.341 | 0.053 | 0.985 | 0.118 |
| 21 | 138.0 | 122.0 | 64.5 | 18.850 | 0.089 | 17.935 | 0.051 | 0.915 | 0.103 |
| 22 | 140.2 | −21.0 | 138.6 | 17.134 | 0.055 | 16.185 | 0.041 | 0.949 | 0.069 |
| 23 | 152.7 | −41.6 | 147.0 | 17.492 | 0.058 | 16.536 | 0.042 | 0.956 | 0.072 |
| 24 | 154.0 | 141.7 | 60.3 | 19.608 | 0.134 | 18.696 | 0.075 | 0.912 | 0.153 |
| 25 | 156.1 | 12.2 | 155.7 | 18.374 | 0.066 | 17.421 | 0.043 | 0.953 | 0.079 |
| 26 | 157.8 | 97.4 | 124.2 | 14.029 | 0.053 | 13.114 | 0.040 | 0.915 | 0.067 |
| 27 | 170.4 | 168.2 | 27.6 | 18.594 | 0.076 | 17.525 | 0.049 | 1.069 | 0.090 |
| 28 | 172.8 | 154.0 | −78.3 | 18.490 | 0.076 | 16.800 | 0.041 | 1.690 | 0.086 |
| 29 | 173.6 | 75.8 | 156.1 | 15.379 | 0.053 | 14.392 | 0.040 | 0.987 | 0.067 |
| 30 | 182.5 | 62.2 | −171.5 | 16.673 | 0.055 | 15.495 | 0.040 | 1.178 | 0.068 |
| 31 | 185.3 | 168.7 | −76.6 | 19.951 | 0.179 | 18.713 | 0.078 | 1.238 | 0.195 |
| 32 | 185.9 | 31.0 | 183.3 | 18.194 | 0.061 | 17.228 | 0.043 | 0.966 | 0.075 |
| 33 | 187.4 | 41.0 | −182.9 | 18.081 | 0.065 | 17.226 | 0.044 | 0.855 | 0.079 |
| 34 | 190.5 | −11.2 | 190.1 | 19.524 | 0.117 | 18.273 | 0.057 | 1.251 | 0.130 |
| 35 | 195.1 | −160.2 | 111.4 | 14.777 | 0.053 | 13.422 | 0.040 | 1.355 | 0.067 |
| 36 | 197.7 | −54.2 | −190.2 | 19.086 | 0.098 | 17.720 | 0.054 | 1.366 | 0.113 |
| 37 | 203.0 | −109.8 | −170.8 | 18.610 | 0.076 | 17.372 | 0.045 | 1.238 | 0.089 |
| 38 | 208.2 | −160.5 | 132.7 | 18.630 | 0.070 | 17.401 | 0.046 | 1.229 | 0.083 |

Notes to Table 8.

Positions relative to $\alpha = 20:53:35$, $\delta = -17:33:54$ (J2000)

# Table 9. EUVE 2114+503

| No. | Sep. | $\Delta\alpha$ | $\Delta\delta$ | $B$ | | $R$ | | $B-R$ | |
|---|---|---|---|---|---|---|---|---|---|
| | arcsec | arcsec | arcsec | mag | $\sigma$ | mag | $\sigma$ | mag | $\sigma$ |
| 1 | 24.2 | −18.6 | −15.5 | 19.829 | 0.028 | 17.178 | 0.018 | 2.651 | 0.033 |
| 2 | 24.3 | −15.0 | −19.1 | 21.909 | 0.122 | 18.697 | 0.023 | 3.212 | 0.124 |
| 3 | 28.3 | −22.1 | −17.7 | 19.637 | 0.025 | 17.225 | 0.019 | 2.412 | 0.032 |
| 4 | 32.1 | −30.3 | −10.6 | 20.992 | 0.053 | 17.925 | 0.020 | 3.067 | 0.057 |
| 5 | 34.5 | 26.2 | −22.5 | 20.075 | 0.043 | 17.303 | 0.019 | 2.772 | 0.047 |
| 6 | 36.3 | −34.0 | 12.8 | 20.517 | 0.038 | 17.579 | 0.019 | 2.938 | 0.043 |
| 7 | 38.2 | −25.5 | 28.5 | 21.493 | 0.102 | 18.505 | 0.022 | 2.988 | 0.104 |
| 8 | 40.8 | 20.6 | 35.2 | 19.703 | 0.027 | 16.857 | 0.018 | 2.846 | 0.033 |
| 9 | 46.2 | −17.8 | 42.7 | 21.311 | 0.092 | 18.172 | 0.021 | 3.139 | 0.094 |
| 10 | 46.8 | 20.0 | −42.3 | 21.092 | 0.064 | 18.053 | 0.021 | 3.039 | 0.067 |
| 11 | 48.2 | −43.9 | 19.9 | 21.251 | 0.078 | 17.298 | 0.019 | 3.953 | 0.080 |
| 12 | 50.0 | 39.3 | 30.9 | 19.761 | 0.029 | 16.887 | 0.019 | 2.874 | 0.035 |
| 13 | 52.8 | −28.3 | −44.6 | 18.728 | 0.020 | 16.124 | 0.018 | 2.604 | 0.027 |
| 14 | 53.4 | 3.4 | 53.3 | 21.303 | 0.075 | 18.220 | 0.023 | 3.083 | 0.079 |
| 15 | 59.2 | −21.3 | −55.2 | 20.789 | 0.053 | 17.675 | 0.021 | 3.114 | 0.057 |
| 16 | 63.9 | −59.9 | 22.4 | 21.473 | 0.098 | 18.554 | 0.022 | 2.919 | 0.100 |
| 17 | 65.2 | 1.2 | −65.2 | 21.744 | 0.132 | 17.886 | 0.020 | 3.858 | 0.134 |
| 18 | 65.9 | 40.3 | 52.1 | 20.616 | 0.041 | 17.570 | 0.020 | 3.046 | 0.046 |
| 19 | 68.2 | 47.5 | −48.9 | 20.631 | 0.047 | 17.402 | 0.019 | 3.229 | 0.050 |
| 20 | 69.3 | 69.3 | −2.9 | 17.188 | 0.018 | 15.090 | 0.018 | 2.098 | 0.026 |
| 21 | 71.2 | 10.3 | −70.4 | 20.659 | 0.044 | 17.691 | 0.019 | 2.968 | 0.048 |
| 22 | 74.6 | −68.3 | −29.9 | 20.792 | 0.069 | 17.156 | 0.020 | 3.636 | 0.072 |
| 23 | 75.9 | −63.8 | 41.1 | 19.644 | 0.032 | 17.239 | 0.020 | 2.405 | 0.038 |
| 24 | 76.3 | −15.5 | 74.7 | 18.802 | 0.020 | 16.282 | 0.018 | 2.520 | 0.027 |
| 25 | 77.9 | −71.2 | −31.7 | 19.538 | 0.028 | 15.299 | 0.018 | 4.239 | 0.034 |
| 26 | 78.4 | −66.2 | 42.0 | 17.156 | 0.019 | 15.152 | 0.018 | 2.004 | 0.026 |
| 27 | 80.0 | 64.4 | 47.5 | 17.861 | 0.019 | 15.242 | 0.018 | 2.619 | 0.026 |
| 28 | 80.6 | 73.9 | −32.2 | 21.458 | 0.118 | 18.552 | 0.022 | 2.906 | 0.120 |
| 29 | 81.1 | 43.3 | 68.6 | 21.437 | 0.072 | 18.297 | 0.025 | 3.140 | 0.076 |
| 30 | 81.8 | −81.8 | 1.9 | 18.371 | 0.019 | 15.753 | 0.018 | 2.618 | 0.026 |
| 31 | 82.0 | 24.0 | −78.4 | 18.348 | 0.022 | 14.368 | 0.020 | 3.980 | 0.030 |
| 32 | 83.4 | −59.8 | 58.2 | 20.383 | 0.041 | 17.383 | 0.020 | 3.000 | 0.046 |
| 33 | 84.1 | −57.0 | 61.8 | 18.481 | 0.019 | 15.998 | 0.018 | 2.483 | 0.027 |
| 34 | 84.7 | −1.8 | 84.6 | 20.213 | 0.037 | 16.335 | 0.018 | 3.878 | 0.041 |
| 35 | 85.6 | −85.6 | −1.3 | 21.706 | 0.119 | 19.013 | 0.029 | 2.693 | 0.123 |
| 36 | 85.8 | 20.6 | −83.3 | 20.458 | 0.039 | 16.083 | 0.018 | 4.375 | 0.043 |
| 37 | 86.6 | −33.1 | 80.0 | 17.919 | 0.019 | 15.431 | 0.018 | 2.488 | 0.026 |
| 38 | 86.8 | 82.5 | 26.9 | 20.095 | 0.035 | 16.243 | 0.018 | 3.852 | 0.039 |
| 39 | 87.0 | −68.0 | 54.3 | 18.428 | 0.019 | 16.186 | 0.018 | 2.242 | 0.027 |
| 40 | 92.1 | −62.9 | 67.4 | 19.636 | 0.028 | 17.287 | 0.018 | 2.349 | 0.034 |
| 41 | 92.2 | −10.7 | 91.6 | 19.216 | 0.022 | 15.272 | 0.018 | 3.944 | 0.028 |
| 42 | 95.0 | 85.8 | 40.6 | 21.659 | 0.119 | 18.623 | 0.026 | 3.036 | 0.122 |
| 43 | 97.3 | 68.2 | 69.4 | 19.676 | 0.025 | 16.703 | 0.018 | 2.973 | 0.031 |
| 44 | 98.0 | −35.9 | 91.2 | 18.690 | 0.022 | 16.147 | 0.018 | 2.543 | 0.028 |
| 45 | 98.7 | 55.3 | −81.8 | 21.550 | 0.101 | 18.293 | 0.021 | 3.257 | 0.103 |
| 46 | 100.6 | −60.3 | 80.6 | 20.459 | 0.037 | 17.530 | 0.019 | 2.929 | 0.041 |

TABLE 9. (continued)

| No. | Sep. | $\Delta\alpha$ | $\Delta\delta$ | $B$ | | $R$ | | $B-R$ | |
|---|---|---|---|---|---|---|---|---|---|
| | arcsec | arcsec | arcsec | mag | $\sigma$ | mag | $\sigma$ | mag | $\sigma$ |
| 47 | 101.3 | −98.2 | −25.0 | 19.484 | 0.026 | 16.886 | 0.019 | 2.598 | 0.032 |
| 48 | 101.4 | 25.0 | −98.3 | 17.373 | 0.018 | 14.805 | 0.018 | 2.568 | 0.026 |
| 49 | 103.1 | −101.7 | −17.4 | 21.298 | 0.075 | 18.203 | 0.021 | 3.095 | 0.078 |
| 50 | 103.9 | −59.3 | −85.3 | 20.659 | 0.049 | 17.580 | 0.019 | 3.079 | 0.053 |
| 51 | 106.4 | −16.3 | −105.2 | 19.960 | 0.037 | 17.230 | 0.019 | 2.730 | 0.041 |
| 52 | 106.5 | 98.6 | −40.2 | 21.474 | 0.101 | 18.493 | 0.022 | 2.981 | 0.103 |
| 53 | 106.8 | 44.9 | 96.9 | 21.906 | 0.140 | 18.765 | 0.023 | 3.141 | 0.142 |
| 54 | 107.5 | 22.7 | −105.1 | 20.364 | 0.041 | 17.342 | 0.020 | 3.022 | 0.046 |
| 55 | 109.0 | 41.4 | −100.9 | 20.581 | 0.048 | 17.857 | 0.020 | 2.724 | 0.052 |
| 56 | 110.4 | 4.0 | −110.3 | 19.028 | 0.022 | 15.248 | 0.018 | 3.780 | 0.029 |
| 57 | 110.6 | 82.8 | 73.4 | 21.467 | 0.101 | 18.252 | 0.021 | 3.215 | 0.103 |
| 58 | 111.7 | 46.0 | −101.8 | 21.048 | 0.069 | 17.716 | 0.019 | 3.332 | 0.072 |
| 59 | 111.9 | −69.5 | −87.7 | 21.135 | 0.058 | 18.208 | 0.021 | 2.927 | 0.062 |
| 60 | 112.3 | −6.9 | 112.1 | 17.538 | 0.020 | 15.155 | 0.018 | 2.383 | 0.027 |
| 61 | 112.4 | −109.7 | −24.6 | 21.794 | 0.115 | 18.795 | 0.022 | 2.999 | 0.118 |
| 62 | 113.8 | 103.4 | 47.5 | 20.049 | 0.032 | 17.225 | 0.020 | 2.824 | 0.038 |
| 63 | 114.3 | 114.1 | −6.8 | 21.747 | 0.111 | 18.708 | 0.026 | 3.039 | 0.114 |
| 64 | 115.0 | −79.7 | −82.9 | 21.933 | 0.152 | 18.349 | 0.022 | 3.584 | 0.154 |
| 65 | 116.6 | 112.8 | −29.8 | 20.525 | 0.052 | 17.632 | 0.019 | 2.893 | 0.056 |
| 66 | 116.7 | 116.1 | −11.8 | 18.113 | 0.019 | 14.557 | 0.018 | 3.556 | 0.026 |
| 67 | 118.9 | −93.4 | 73.6 | 18.792 | 0.020 | 15.206 | 0.018 | 3.586 | 0.027 |
| 68 | 121.0 | −116.1 | 34.0 | 20.502 | 0.047 | 17.599 | 0.020 | 2.903 | 0.051 |
| 69 | 124.3 | 48.7 | 114.4 | 19.121 | 0.021 | 16.574 | 0.018 | 2.547 | 0.028 |
| 70 | 124.8 | 40.0 | −118.2 | 20.793 | 0.052 | 17.767 | 0.019 | 3.026 | 0.056 |
| 71 | 125.0 | −0.3 | 125.0 | 21.043 | 0.069 | 17.937 | 0.021 | 3.106 | 0.072 |
| 72 | 125.7 | 31.6 | 121.7 | 19.026 | 0.023 | 16.401 | 0.018 | 2.625 | 0.030 |
| 73 | 128.1 | −67.4 | −108.8 | 19.682 | 0.028 | 17.028 | 0.018 | 2.654 | 0.034 |
| 74 | 129.0 | −74.0 | −105.7 | 21.647 | 0.103 | 18.363 | 0.021 | 3.284 | 0.105 |
| 75 | 130.2 | 123.2 | 42.0 | 20.613 | 0.048 | 17.639 | 0.019 | 2.974 | 0.052 |
| 76 | 130.3 | −0.4 | −130.3 | 18.090 | 0.020 | 15.580 | 0.018 | 2.510 | 0.027 |
| 77 | 131.7 | 125.7 | −39.2 | 21.286 | 0.083 | 18.163 | 0.021 | 3.123 | 0.086 |
| 78 | 132.1 | 127.8 | −33.3 | 19.178 | 0.023 | 19.036 | 0.025 | 0.142 | 0.034 |
| 79 | 132.2 | 131.0 | −18.0 | 20.083 | 0.034 | 15.688 | 0.018 | 4.395 | 0.039 |
| 80 | 133.7 | −44.8 | 126.0 | 19.815 | 0.028 | 16.036 | 0.018 | 3.779 | 0.034 |
| 81 | 133.9 | −71.8 | −113.1 | 21.876 | 0.116 | 18.718 | 0.024 | 3.158 | 0.119 |
| 82 | 135.2 | −77.4 | 110.9 | 19.027 | 0.020 | 16.272 | 0.018 | 2.755 | 0.027 |
| 83 | 138.4 | −138.1 | −9.8 | 19.198 | 0.022 | 16.873 | 0.018 | 2.325 | 0.028 |
| 84 | 140.8 | −131.4 | −50.6 | 20.409 | 0.034 | 17.670 | 0.020 | 2.739 | 0.040 |
| 85 | 141.5 | 32.3 | −137.8 | 20.675 | 0.061 | 17.969 | 0.020 | 2.706 | 0.064 |
| 86 | 141.6 | −14.8 | −140.9 | 21.590 | 0.108 | 17.497 | 0.019 | 4.093 | 0.109 |
| 87 | 143.1 | 14.9 | −142.4 | 20.549 | 0.047 | 17.895 | 0.020 | 2.654 | 0.051 |
| 88 | 143.4 | 118.0 | −81.3 | 22.086 | 0.165 | 18.428 | 0.023 | 3.658 | 0.167 |
| 89 | 143.9 | −114.1 | −87.7 | 19.656 | 0.027 | 16.657 | 0.018 | 2.999 | 0.033 |
| 90 | 145.0 | −128.6 | 67.2 | 21.900 | 0.135 | 19.098 | 0.024 | 2.802 | 0.137 |
| 91 | 148.1 | 86.1 | 120.5 | 18.096 | 0.019 | 15.797 | 0.018 | 2.299 | 0.026 |
| 92 | 148.2 | −115.4 | −92.9 | 19.764 | 0.029 | 17.045 | 0.018 | 2.719 | 0.035 |

TABLE 9. (continued)

| No. | Sep. | $\Delta\alpha$ | $\Delta\delta$ | $B$ | | $R$ | | $B-R$ | |
|---|---|---|---|---|---|---|---|---|---|
| | arcsec | arcsec | arcsec | mag | $\sigma$ | mag | $\sigma$ | mag | $\sigma$ |
| 93 | 149.2 | 26.0 | −146.9 | 22.251 | 0.242 | 19.179 | 0.028 | 3.072 | 0.243 |
| 94 | 149.5 | 147.9 | −21.3 | 21.632 | 0.106 | 17.490 | 0.019 | 4.142 | 0.107 |
| 95 | 149.9 | −149.8 | −3.9 | 18.197 | 0.019 | 14.858 | 0.018 | 3.339 | 0.026 |
| 96 | 150.1 | 150.1 | −1.8 | 20.539 | 0.048 | 17.605 | 0.019 | 2.934 | 0.051 |
| 97 | 152.3 | −117.4 | 97.1 | 21.650 | 0.132 | 18.748 | 0.025 | 2.902 | 0.135 |
| 98 | 153.5 | −34.5 | 149.6 | 20.840 | 0.044 | 17.904 | 0.020 | 2.936 | 0.048 |
| 99 | 153.7 | 147.9 | −41.8 | 19.989 | 0.026 | 16.900 | 0.018 | 3.089 | 0.032 |
| 100 | 154.0 | 87.4 | 126.8 | 21.720 | 0.105 | 18.463 | 0.023 | 3.257 | 0.107 |
| 101 | 155.3 | 23.8 | −153.5 | 21.017 | 0.075 | 18.341 | 0.022 | 2.676 | 0.078 |
| 102 | 156.4 | 156.4 | −3.7 | 21.018 | 0.061 | 18.438 | 0.022 | 2.580 | 0.065 |
| 103 | 156.8 | −107.7 | 114.0 | 22.244 | 0.195 | 18.889 | 0.027 | 3.355 | 0.197 |
| 104 | 158.2 | 148.1 | −55.6 | 19.108 | 0.022 | 16.235 | 0.018 | 2.873 | 0.029 |
| 105 | 158.8 | −157.2 | −22.0 | 21.773 | 0.127 | 18.787 | 0.046 | 2.986 | 0.135 |
| 106 | 160.1 | 140.1 | 77.6 | 20.873 | 0.060 | 17.664 | 0.019 | 3.209 | 0.063 |
| 107 | 162.5 | 41.6 | 157.1 | 21.438 | 0.227 | 18.627 | 0.023 | 2.811 | 0.228 |
| 108 | 162.8 | −143.2 | 77.5 | 20.724 | 0.044 | 17.547 | 0.021 | 3.177 | 0.048 |
| 109 | 163.3 | 163.1 | 8.1 | 19.934 | 0.028 | 17.149 | 0.019 | 2.785 | 0.034 |
| 110 | 164.0 | 36.4 | 159.9 | 21.737 | 0.123 | 18.509 | 0.022 | 3.228 | 0.125 |
| 111 | 164.3 | −68.6 | −149.3 | 22.064 | 0.183 | 18.749 | 0.024 | 3.315 | 0.184 |
| 112 | 164.8 | −157.1 | −49.7 | 20.852 | 0.062 | 18.427 | 0.047 | 2.425 | 0.077 |
| 113 | 165.3 | −109.5 | 123.9 | 20.476 | 0.039 | 17.613 | 0.022 | 2.863 | 0.045 |
| 114 | 167.7 | 113.7 | 123.3 | 21.025 | 0.066 | 17.986 | 0.020 | 3.039 | 0.068 |
| 115 | 167.8 | −115.6 | 121.7 | 20.948 | 0.059 | 17.781 | 0.019 | 3.167 | 0.062 |
| 116 | 170.0 | −85.0 | 147.2 | 20.844 | 0.063 | 17.972 | 0.020 | 2.872 | 0.066 |
| 117 | 170.1 | −15.4 | 169.4 | 21.913 | 0.105 | 18.157 | 0.019 | 3.756 | 0.106 |
| 118 | 170.5 | −26.9 | 168.3 | 18.018 | 0.019 | 15.603 | 0.018 | 2.415 | 0.026 |
| 119 | 171.1 | −16.2 | −170.3 | 19.800 | 0.026 | 17.371 | 0.019 | 2.429 | 0.032 |
| 120 | 171.5 | −140.3 | −98.7 | 21.776 | 0.138 | 18.567 | 0.022 | 3.209 | 0.140 |
| 121 | 171.9 | −154.7 | −74.8 | 21.064 | 0.065 | 18.039 | 0.022 | 3.025 | 0.068 |
| 122 | 173.1 | −160.2 | −65.6 | 21.764 | 0.120 | 18.652 | 0.024 | 3.112 | 0.123 |
| 123 | 173.3 | 161.6 | 62.7 | 20.123 | 0.034 | 16.861 | 0.018 | 3.262 | 0.039 |
| 124 | 173.6 | 161.9 | −62.6 | 21.615 | 0.119 | 18.305 | 0.023 | 3.310 | 0.122 |
| 125 | 175.2 | 138.3 | 107.6 | 21.506 | 0.082 | 18.501 | 0.022 | 3.005 | 0.085 |
| 126 | 175.9 | −106.1 | 140.3 | 18.038 | 0.020 | 15.472 | 0.018 | 2.566 | 0.027 |
| 127 | 176.0 | −26.2 | 174.1 | 21.127 | 0.077 | 18.303 | 0.022 | 2.824 | 0.080 |
| 128 | 176.5 | 150.7 | 91.8 | 17.661 | 0.019 | 15.498 | 0.018 | 2.163 | 0.026 |
| 129 | 177.7 | −89.4 | −153.6 | 21.298 | 0.089 | 18.610 | 0.025 | 2.688 | 0.092 |
| 130 | 178.1 | −79.7 | −159.2 | 22.119 | 0.204 | 19.085 | 0.038 | 3.034 | 0.207 |
| 131 | 178.4 | 175.9 | 30.1 | 21.285 | 0.077 | 18.209 | 0.020 | 3.076 | 0.080 |
| 132 | 179.0 | −178.3 | −15.9 | 17.632 | 0.019 | 14.770 | 0.018 | 2.862 | 0.026 |
| 133 | 179.1 | −43.4 | 173.7 | 18.576 | 0.020 | 15.922 | 0.018 | 2.654 | 0.027 |
| 134 | 179.1 | −133.0 | 120.0 | 20.929 | 0.064 | 18.115 | 0.021 | 2.814 | 0.067 |
| 135 | 179.3 | −152.4 | −94.3 | 19.448 | 0.024 | 17.048 | 0.019 | 2.400 | 0.030 |
| 136 | 180.3 | −155.6 | −90.9 | 20.345 | 0.038 | 17.398 | 0.019 | 2.947 | 0.042 |
| 137 | 180.4 | 102.9 | 148.2 | 19.660 | 0.032 | 16.814 | 0.018 | 2.846 | 0.037 |
| 138 | 180.6 | 84.9 | 159.4 | 18.916 | 0.022 | 16.237 | 0.018 | 2.679 | 0.029 |

TABLE 9. (continued)

| No. | Sep. | $\Delta\alpha$ | $\Delta\delta$ | $B$ | | $R$ | | $B-R$ | |
|---|---|---|---|---|---|---|---|---|---|
| | arcsec | arcsec | arcsec | mag | $\sigma$ | mag | $\sigma$ | mag | $\sigma$ |
| 139 | 181.1 | 172.0 | 56.9 | 21.828 | 0.164 | 18.793 | 0.026 | 3.035 | 0.166 |
| 140 | 182.8 | 182.7 | 6.7 | 21.777 | 0.135 | 18.906 | 0.025 | 2.871 | 0.138 |
| 141 | 183.1 | 10.8 | −182.8 | 20.994 | 0.056 | 17.278 | 0.019 | 3.716 | 0.059 |
| 142 | 186.5 | −134.1 | 129.6 | 20.810 | 0.052 | 17.582 | 0.019 | 3.228 | 0.056 |
| 143 | 186.8 | 186.0 | −17.6 | 20.990 | 0.051 | 17.824 | 0.022 | 3.166 | 0.056 |
| 144 | 187.9 | −184.2 | 37.1 | 18.432 | 0.019 | 15.886 | 0.018 | 2.546 | 0.027 |
| 145 | 189.2 | 26.4 | 187.4 | 19.385 | 0.025 | 16.750 | 0.018 | 2.635 | 0.031 |
| 146 | 189.5 | −117.7 | 148.5 | 20.407 | 0.038 | 17.351 | 0.019 | 3.056 | 0.042 |
| 147 | 192.0 | −189.0 | −33.3 | 21.118 | 0.071 | 17.946 | 0.021 | 3.172 | 0.074 |
| 148 | 192.3 | 155.6 | −113.0 | 20.799 | 0.048 | 17.585 | 0.019 | 3.214 | 0.052 |
| 149 | 192.9 | 80.5 | −175.3 | 20.394 | 0.042 | 17.311 | 0.019 | 3.083 | 0.046 |
| 150 | 193.9 | −87.0 | −173.3 | 18.357 | 0.020 | 15.814 | 0.018 | 2.543 | 0.027 |
| 151 | 197.7 | 126.0 | −152.3 | 21.215 | 0.075 | 17.735 | 0.020 | 3.480 | 0.078 |
| 152 | 198.0 | −28.6 | −195.9 | 18.943 | 0.023 | 16.181 | 0.018 | 2.762 | 0.030 |
| 153 | 198.3 | 21.2 | 197.2 | 20.530 | 0.048 | 17.860 | 0.019 | 2.670 | 0.052 |
| 154 | 198.7 | 192.5 | 49.5 | 21.827 | 0.101 | 18.953 | 0.026 | 2.874 | 0.104 |
| 155 | 199.6 | 64.0 | −189.0 | 21.234 | 0.080 | 17.928 | 0.021 | 3.306 | 0.083 |
| 156 | 199.8 | −192.1 | −54.9 | 20.951 | 0.073 | 18.285 | 0.022 | 2.666 | 0.076 |
| 157 | 202.3 | −202.3 | −0.8 | 21.608 | 0.105 | 18.597 | 0.025 | 3.011 | 0.107 |
| 158 | 203.5 | −58.6 | −194.8 | 20.855 | 0.062 | 17.751 | 0.019 | 3.104 | 0.065 |
| 159 | 203.8 | −154.9 | 132.4 | 20.398 | 0.040 | 17.661 | 0.020 | 2.737 | 0.045 |
| 160 | 204.1 | −194.5 | 62.1 | 19.674 | 0.023 | 15.519 | 0.018 | 4.155 | 0.030 |
| 161 | 204.8 | 117.3 | 168.0 | 20.468 | 0.043 | 17.558 | 0.019 | 2.910 | 0.047 |
| 162 | 205.8 | −137.0 | 153.7 | 19.815 | 0.024 | 16.081 | 0.018 | 3.734 | 0.030 |
| 163 | 205.8 | −186.3 | −87.5 | 21.429 | 0.086 | 18.393 | 0.022 | 3.036 | 0.089 |
| 164 | 206.3 | 163.2 | 126.3 | 21.682 | 0.110 | 18.631 | 0.025 | 3.051 | 0.113 |
| 165 | 207.2 | 53.7 | 200.1 | 21.859 | 0.116 | 19.188 | 0.029 | 2.671 | 0.120 |
| 166 | 207.9 | −133.4 | −159.4 | 16.603 | 0.028 | 14.686 | 0.019 | 1.917 | 0.034 |
| 167 | 208.2 | −72.0 | 195.3 | 20.052 | 0.031 | 17.243 | 0.019 | 2.809 | 0.036 |
| 168 | 209.4 | −124.8 | 168.2 | 17.107 | 0.019 | 14.766 | 0.018 | 2.341 | 0.026 |
| 169 | 210.3 | 10.3 | 210.1 | 19.415 | 0.024 | 17.131 | 0.019 | 2.284 | 0.030 |

Notes to Table 9.

Positions relative to $\alpha = 21:14:41$, $\delta = +50:18:12$ (J2000)

## TABLE 10. RE 2303+212

| No. | Sep. | $\Delta\alpha$ | $\Delta\delta$ | $B$ | | $R$ | | $B-R$ | |
|---|---|---|---|---|---|---|---|---|---|
| | arcsec | arcsec | arcsec | mag | $\sigma$ | mag | $\sigma$ | mag | $\sigma$ |
| 1 | 20.3 | 14.5 | 14.1 | 21.318 | 0.186 | 19.692 | 0.045 | 1.626 | 0.191 |
| 2 | 76.3 | 69.6 | 31.3 | 20.189 | 0.063 | 18.330 | 0.024 | 1.859 | 0.067 |
| 3 | 78.6 | −76.4 | −18.5 | 16.057 | 0.018 | 14.531 | 0.018 | 1.526 | 0.026 |
| 4 | 83.8 | 54.2 | 63.9 | 20.260 | 0.065 | 17.663 | 0.021 | 2.597 | 0.068 |
| 5 | 84.4 | 44.6 | −71.7 | 18.847 | 0.029 | 17.045 | 0.020 | 1.802 | 0.035 |
| 6 | 102.1 | −82.3 | −60.5 | 19.512 | 0.034 | 16.903 | 0.020 | 2.609 | 0.039 |
| 7 | 119.8 | 76.6 | −92.1 | 18.435 | 0.025 | 16.686 | 0.019 | 1.749 | 0.031 |
| 8 | 133.5 | −47.2 | 124.9 | 19.888 | 0.048 | 17.766 | 0.021 | 2.122 | 0.052 |
| 9 | 160.6 | 53.6 | −151.3 | 16.122 | 0.019 | 14.696 | 0.018 | 1.426 | 0.026 |
| 10 | 169.3 | −124.5 | −114.8 | 20.512 | 0.063 | 18.415 | 0.025 | 2.097 | 0.067 |
| 11 | 178.5 | 84.8 | 157.1 | 20.228 | 0.071 | 18.069 | 0.022 | 2.159 | 0.075 |
| 12 | 184.3 | −75.6 | 168.0 | 19.370 | 0.033 | 17.150 | 0.021 | 2.220 | 0.039 |
| 13 | 198.8 | 189.3 | −60.6 | 16.186 | 0.019 | 14.295 | 0.018 | 1.891 | 0.026 |
| 14 | 207.1 | -207.1 | 1.2 | 12.324 | 0.010 | 10.200 | 0.3 | 2.1 | 0.3 |
| 15 | 208.9 | −199.7 | 61.5 | 18.555 | 0.028 | 16.809 | 0.019 | 1.746 | 0.034 |

Notes to Table 10.

Positions relative to $\alpha = 23:03:04$, $\delta = +21:20:32$ (J2000)

# TABLE 11. X-ray Visibility of EUV-Detected Cataclysmic Variables

| Name | Type | *EUVE* | | | | *Rosat* | | X-Ray |
|---|---|---|---|---|---|---|---|---|
| | | 100Å | 200Å | 400Å | 600Å | 100Å | 150Å | Instrument |
| BL Hyi | AM Her | 52± 7 | ··· | ··· | ··· | 257± 19 | 211± 17 | IPC |
| EF Eri | AM Her | 419± 21 | ··· | ··· | ··· | 195± 20 | 266± 28 | IPC |
| UZ For | AM Her | 1156± 732 | ··· | ··· | ··· | ··· | ··· | PSPC |
| VW Hyi | SU UMa | 16± 3 | 13± 5 | 19± 7 | ··· | 17± 4 | 25± 6 | IPC |
| RE0453-421 | AM Her | 44± 8 | ··· | ··· | ··· | 53± 9 | 18± 7 | PSPC |
| RE0531-46 | AM Her | ··· | ··· | ··· | ··· | 20± 4 | ··· | PSPC |
| PQ Gem | DQ Her | ··· | ··· | ··· | ··· | 19± 4 | ··· | PSPC |
| VV Pup | Nova-like | ··· | ··· | ··· | ··· | 248± 15 | 282± 16 | IPC |
| IX Vel | Nova-like | 6.7⋆ | ··· | ··· | ··· | 11± 3 | 33± 5 | PSPC |
| EK UMa | AM Her | 63± 11 | ··· | ··· | ··· | 33± 6 | ··· | IPC |
| AN UMa | AM Her | 211± 16 | ··· | ··· | ··· | 180± 11 | 262± 16 | IPC |
| US 3019 | AM Her | 103± 19 | ··· | 82± 41 | ··· | 149± 11 | 112± 10 | ··· |
| EX Hya | DQ Her | 82± 12 | ··· | ··· | ··· | 58± 9 | 51± 10 | IPC, PSPC, HEAO1 |
| RE1307+53 | AM Her | ··· | ··· | ··· | ··· | 54± 7 | 28± 5 | ··· |
| V834 Cen | AM Her | 282± 20 | ··· | ··· | ··· | ··· | ··· | PSPC |
| EUVE1429-380 | AM Her | 4.2 | ··· | ··· | ··· | ··· | ··· | ··· |
| AM Her | AM Her | 4233± 36 | 94± 9 | ··· | ··· | ··· | ··· | PSPC |
| RE1844-74 | AM Her | 150± 11 | ··· | ··· | 93± 34 | 117± 22 | 74± 23 | PSPC |
| RE1938-46 | AM Her | 142± 15 | ··· | ··· | ··· | 424± 21 | 302± 18 | IPC |
| QQ Vul | AM Her | 286± 25 | ··· | ··· | ··· | 454± 19 | 147± 13 | IPC, PSPC |
| V1974 Cyg | Nova | 129± 11 | 92± 14 | 30± 13 | ··· | ··· | ··· | PSPC |
| RE2107-05 | AM Her | ··· | ··· | ··· | ··· | 24± 5 | ··· | PSPC |
| EUVE2115-586 | AM Her | 59± 12 | 31± 12 | ··· | ··· | ··· | ··· | ··· |
| SS Cyg | U Gem | 1044.6⋆ | ··· | ··· | ··· | 375± 13 | 61± 6 | IPC, HEAO1 |

Notes to Table 11.

Entries are counts ksec$^{-1}$ in given EUV band. Identification with X-ray sources are based on positional coincidence within 1.1′. Instrument abbreviations: IPC – *Einstein IPC*; PSPC – *Rosat PSPC*; ⋆ – *EUVE* observation with the Deep Survey Telescope.